Genetic Variants in Telomerase Reverse Transcriptase Contribute to Solar Lentigines

JID Open

Qianqian Peng[1,14], Yu Liu[1,14], Anke Huels[2,3], Canfeng Zhang[4], Yao Yu[1,5], Wenqing Qiu[6], Xiyang Cai[1], Yuepu Zhao[1], Tamara Schikowski[2], Katja Merches[2], Yun Liu[6], Yajun Yang[7,8], Jiucun Wang[7,8], Yong Zhao[9], Li Jin[7,8], Liang Zhang[5,10,11], Jean Krutmann[2,7,12,14] and Sijia Wang[1,13,14]

Solar lentigines (SLs) are a hallmark of human skin aging. They result from chronic exposure to sunlight and other environmental stressors. Recent studies also imply genetic factors, but findings are partially conflicting and lack of replication. Through a multi-trait based analysis strategy, we discovered that genetic variants in telomerase reverse transcriptase were significantly associated with non-facial SL in two East Asian (Taizhou longitudinal cohort, n = 2,964 and National Survey of Physical Traits, n = 2,954) and one Caucasian population (SALIA, n = 462), top SNP rs2853672 (*P*-value for Taizhou longitudinal cohort = 1.32×10^{-28} and *P*-value for National Survey of Physical Traits = 3.66×10^{-17} and *P*-value for SALIA = 0.0007 and $P_{meta} = 4.93 \times 10^{-44}$). The same variants were nominally associated with facial SL but not with other skin aging or skin pigmentation traits. The SL-enhanced allele/haplotype upregulated the transcription of the telomerase reverse transcriptase gene. Of note, well-known telomerase reverse transcriptase–related aging markers such as leukocyte telomere length and intrinsic epigenetic age acceleration were not associated with SL. Our results indicate a previously unrecognized role of telomerase reverse transcriptase in skin aging–related lentigines formation.

Journal of Investigative Dermatology (2023) **143,** 1062–1072; doi:10.1016/j.jid.2022.11.016

[1]*CAS Key Laboratory of Computational Biology, Shanghai Institute of Nutrition and Health, University of Chinese Academy of Sciences, Chinese Academy of Sciences, Shanghai, China;* [2]*IUF - Leibniz Research Institute for Environmental Medicine, Düsseldorf, Germany;* [3]*Faculty of Epidemiology, Rollins School of Public Health, Emory University, Atlanta, Georgia, USA;* [4]*Scientific Research Center, The Seventh Affiliated Hospital, Sun Yat-Sen University, Shenzhen, China;* [5]*CAS Key Laboratory of Tissue Microenvironment and Tumor, Shanghai Institute of Nutrition and Health, University of Chinese Academy of Sciences, Chinese Academy of Sciences, Shanghai, China;* [6]*MOE Key Laboratory of Metabolism and Molecular Medicine, Department of Biochemistry and Molecular Biology, School of Basic Medical Sciences, Fudan University, Shanghai, China;* [7]*State Key Laboratory of Genetic Engineering, Collaborative Innovation Center for Genetics and Development, Human Phenome Institute, Fudan University, Shanghai, China;* [8]*Ministry of Education Key Laboratory of Contemporary Anthropology, Department of Anthropology and Human Genetics, School of Life Sciences, Fudan University, Shanghai, China;* [9]*Key Laboratory of Gene Engineering of the Ministry of Education, School of Life Sciences, Sun Yat-sen University, Guangzhou, China;* [10]*Institute for Stem Cell and Regeneration, Chinese Academy of Sciences, Beijing, China;* [11]*Department of Plastic and Reconstructive Surgery, Shanghai Ninth People's Hospital, Shanghai Jiao Tong University School of Medicine, Shanghai, China;* [12]*Medical Faculty, Heinrich-Heine-University, Düsseldorf, Germany; and* [13]*Center for Excellence in Animal Evolution and Genetics, Chinese Academy of Sciences, Kunming, China*

[14]*These authors contributed equally to this work.*

Correspondence: Sijia Wang, CAS Key Laboratory of Computational Biology, Shanghai Institute of Nutrition and Health, University of Chinese Academy of Sciences, Chinese Academy of Sciences, 320 Yueyang Road, Shanghai 200030, China. E-mail: wangsijia@picb.ac.cn

Abbreviations: IEAA, intrinsic epigenetic age acceleration; LTL, leukocyte telomere length; MAF, minor allele frequency; NSPT, National Survey of Physical Traits; PLSPM, partial least square path model; SL, solar lentigines; TERT, telomerase reverse transcriptase; TZL, Taizhou longitudinal cohort

Received 21 December 2021; revised 1 October 2022; accepted 11 November 2022; accepted manuscript published online 24 December 2022; corrected proof published online 12 January 2023

INTRODUCTION

Solar lentigines (SL), also called age spots or senile lentigines, are a typical dyspigmentation phenotype in aged skin (Ezzedine et al., 2013; Hasegawa et al., 2015). These hyperpigmented (dark brown) maculae are acquired and evolve slowly over years in sun-exposed areas of the skin such as the face, but also non-facial skin, that is, the dorsal side of the hands and arms (Ezzedine et al., 2013). As indicated by their name, SL are thought to mainly result from chronic irradiation with UVR (Ezzedine et al., 2013). More recently, chronic exposure to other environmental stressors such as air pollutants was also found to be associated with more facial lentigines (Grether-Beck et al., 2021; Hüls et al., 2016; Vierkötter et al., 2010). In addition to these environmental factors, SL also have a substantial genetic component, with a reported 41% heritability (Gunn et al., 2009). Although recent GWASs have detected a number of genetic variants associated with SL (Endo et al., 2018; Jacobs et al., 2015; Laville et al., 2016; Shin et al., 2021), most signals were not replicated in other studies. Ethnic differences may play a role, but even within the same ethnic group, the between-study replication performance remained poor.

It is worth pointing out that in the past, GWASs exclusively focused on facial SL and largely ignored non-facial SL. Compared with facial SL, non-facial SL might offer some advantages for the design of a genetic study. Accordingly, the phenotyping of non-facial SL might be less confounded by other pigmented, maculous lesions such as freckles, seborrheic keratosis, junctional nevomelanocytic nevi, pigmented actinic keratosis, and others, which might also occur in the face (Jacobs et al., 2015). Compared with facial SL, non-facial SL should also be less affected by the regular use of cosmetic day care products,

which are usually applied to the face. Although a comprehensive study of 190 SL obtained from a total of 98 patients recently reported histopathological differences between facial and non-facial SL (Barysch et al., 2019), a direct comparison of facial and non-facial SL has never been conducted in a genetic study.

In this study, we therefore sought to reassess the genetic basis of SL by (i) simultaneously studying non-facial and facial SL, (ii) in two Han Chinese cohorts and one Caucasian cohort, and (iii) by using multi-trait analysis strategies to increase the sensitivity of GWAS. Because three non-facial SL and four facial SL traits were collected in this study, a partial least square path model (PLSPM) was applied to extract composite phenotypes from these traits. This multi-trait-based approach relieved the burden of multiple testing and enhanced the power of GWAS. This approach allowed us to discover an unreported contribution of telomerase reverse transcriptase gene (*TERT*) to SL.

RESULTS

Multi-trait based GWAS identified non-facial SL associated signal at 5p15.33

The correlation matrix of the seven SL traits showed two clear clusters: the three non-facial SL traits collected from the backside of hands and arms (Supplementary Figure S1) were correlated with themselves in one cluster, whereas the four facial SL traits were correlated in the other cluster (Supplementary Figure S2a and Supplementary Table S1). Using a PLSPM, we were able to extract two latent variables, which we denoted as composite phenotypes of non-facial SL and facial SL, respectively (Figure 1a and Supplementary Figure S2b). The composite phenotypes showed slightly to moderately higher heritability than the corresponding single traits (32 ± 13% vs. 21 ± 13% ~ 36 ± 13% for non-facial SL, 36 ± 11% vs. 16 ± 12% ~ 33 ± 12% for facial SL in the Taizhou longitudinal cohort [TZL]; 42 ± 8% vs. 38 ± 8% ~ 44 ± 8% for non-facial SL, 43 ± 8% vs. 26 ± 9% ~ 40 ± 8% for facial SL in National Survey of Physical Traits [NSPT]) (Supplementary Table S2). This indicates that the shared genetic basis of the single traits has been extracted into the composite phenotypes, which might potentially enhance the power of GWAS.

Subsequent genome-wide scans in the two Han Chinese discovery cohorts (TZL and NSPT) found no signal for the composite phenotype of facial SL but two signals for non-facial SL (top SNP rs2853672 at 5p15.33, $\beta = -0.19$, $P_{meta} = 5.68 \times 10^{-42}$; top SNP rs1800414 at 15q12, $\beta = -0.08$, $P_{meta} = 4.67 \times 10^{-8}$) (Figure 1b). The top SNP rs1800414 at

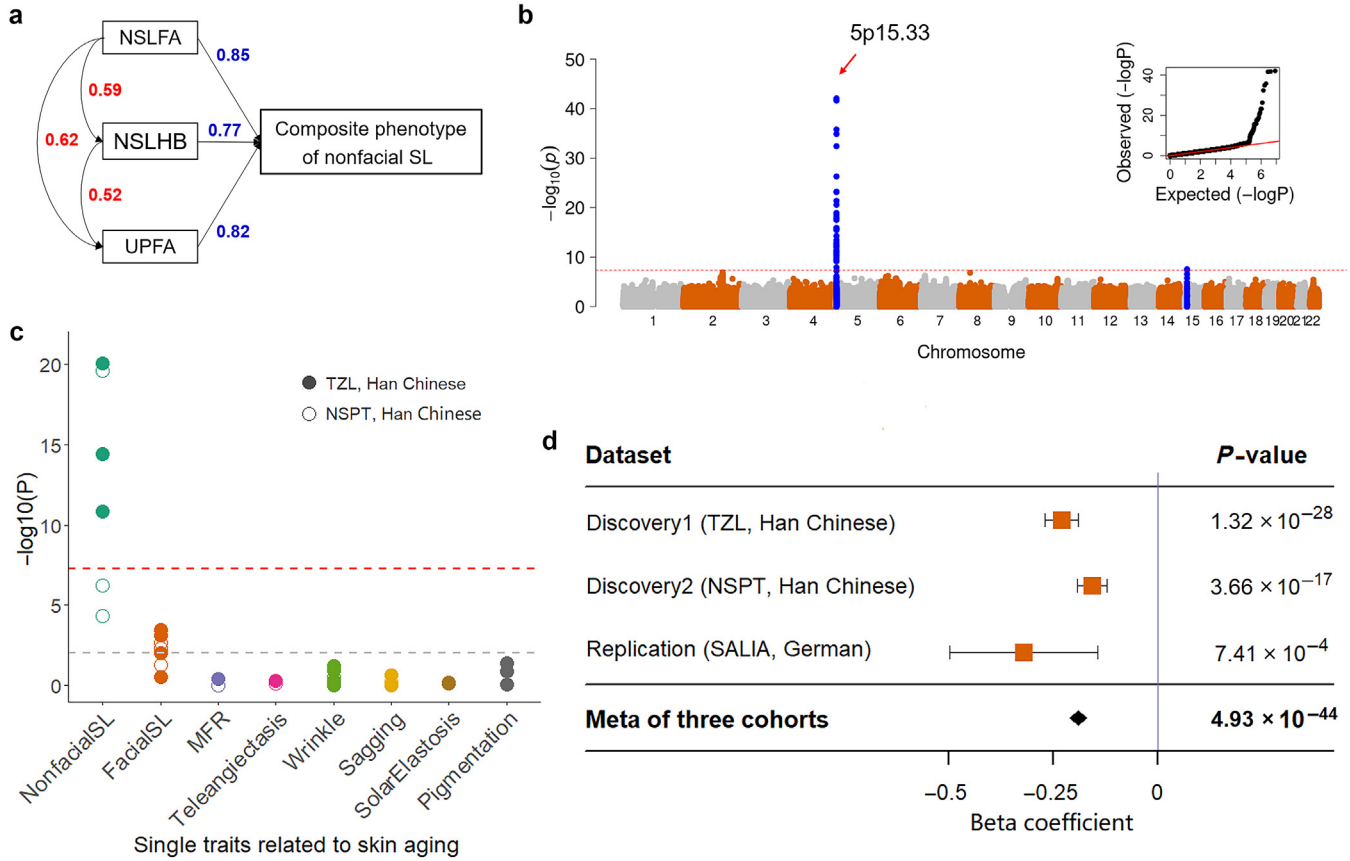

Figure 1. GWAS and meta results of non-facial SL. (**a**) Non-facial SL composite phenotype extraction. Numbers in red indicate correlation coefficients among three single traits, and numbers in blue indicate loading coefficients in PLSPM. (**b**) Meta-result from two Han Chinese samples (TZL and NSPT). Blue dots indicate signals ($P < 5.0 \times 10^{-8}$). (**c**) Association between top SNP rs2853672 and skin aging and pigmentation traits. Colors represent the types of traits, solid dots represent the associations in TZL, and hollow dots represent the associations in NSPT. (**d**) Association between rs2853672 and non-facial SL composite phenotype in two discovery cohorts (TZL and NSPT), one replication cohort (SALIA), and meta-result of three cohorts. The square with black lines indicates a beta-coefficient and 95% CI in each cohort, whereas the rhombus indicates a beta-coefficient in the meta-analysis of three cohorts. CI, confidence interval; NSLFA, SL on forearm; NSLHB SL on back of hands; NSPT, National Survey of Physical Traits; PLSPM, partial least square path model; SL, solar lentigines; TZL, Taizhou longitudinal cohort; UPFA, uneven pigmentation on the lower side of the forearm.

15q12 is a well-known missense variant in *OCA2* previously reported to be associated with skin pigmentation in East Asians (Eaton et al., 2015; Edwards et al., 2010; Murray et al., 2015; Rawofi et al., 2017; Yang et al., 2016). The signal at 5p15.33 is an unreported discovery that has never been reported by previous SL-related genetic studies. We replicated this finding in a German cohort (SALIA, n = 462, $\beta = -0.32$, $P = 7.41 \times 10^{-4}$) (Supplementary Table S3). A meta-analysis combining the GWAS results of all three cohorts showed a greater significance of the signal ($\beta = -0.19$, $P_{meta} = 4.93 \times 10^{-44}$) (Figure 1d and Supplementary Table S3). This signal is located in *TERT*, and the top SNP, rs2853672, could explain 2.95% variance of non-facial SL.

This signal in *TERT* also appeared in the GWAS on the three single traits of non-facial SL but with less significant *P*-values, and was nominally associated with the composite phenotype and single traits of facial SL (Figure 1c). However, it was not associated with any of the other skin aging traits (e.g., wrinkles, sagging, and solar elastosis) (Figure 1c) in the two East Asian cohorts (TZL and NSPT). Furthermore, this signal was also not associated with skin pigmentation phenotypes (Figure 1c). Its association with SL remained significant after adjusting for skin pigmentation (Supplementary Table S4). When exploring the association between *TERT* SNPs and non-facial SL in dark and light skin color groups in TZL and NSPT, no obvious difference was detected between the two groups (Supplementary Table S5), indicating that the effect of *TERT* SNPs on SL should be irrelevant to skin pigmentation.

Previous GWASs on facial SL had reported 29 signal SNPs in European and East Asian populations (Endo et al., 2018; Jacobs et al., 2015; Laville et al., 2016; Shin et al., 2021). None of the 13 SNPs reported in European studies were significant in our Han Chinese samples, probably because most SNPs have very low minor allele frequencies in East Asians (Supplementary Table S6). In contrast, 11 of the 16 SNPs reported in East Asian studies were also nominally significant ($P < 0.05$) in our Han Chinese samples, with consistent effect direction (seven remained significant after multiple testing corrections). This indicates that previously detected genetic variants associated with SL show a strong population difference in allele frequencies. This is probably due to the fact that these variants are located in pigmentation-related genes, which have undergone varied selections in different populations, resulting in the difference in allele frequencies (Adhikari et al., 2019; Feng et al., 2021; Jonnalagadda et al., 2022; Ju and Mathieson, 2021; Rocha, 2020; Yang et al., 2018). However, the signal in *TERT* identified in this study appears to have not been subjected to selection in different populations, for example, with similar allele frequency in different populations. This may be the reason why the *TERT* signal could be found in both East Asian and European populations. Interestingly, in our data, these previously reported candidate SNPs were in general more significantly associated with non-facial SL than with facial SL, further supporting our assumption that studying non-facial SL might be more efficient in genetic studies.

SL-enhanced alleles/haplotypes upregulate *TERT*

Using two different fine mapping strategies, that is, PAINTOR (Probabilistic Annotation INTegratOR) (Kichaev et al., 2014) and Integrative Weighted scoring (Wang et al., 2018), we obtained five candidate SNPs at 5p15.33 (Figure 2a). Although there are a number of luciferase reporter experiments on *TERT* SNPs (e.g., rs2853669, rs2736940) and sequence variations (Helbig et al., 2017; Ko et al., 2016; Ma et al., 2019; Sheng et al., 2013), none of them involved rs2853672, rs2736098, and rs7712562. To identify the most likely causal SNPs and their role in *TERT* expression, we designed luciferase reporter experiments on both allele and haplotype levels for five candidate SNPs. Interestingly, the haplotype consisting of five SL-enhanced alleles was also the most frequent haplotype, and it was significantly associated with SL when compared with other haplotypes (Figure 2b and Supplementary Table S7). *TERT* luciferase reporter assays for this haplotype consisting of five SL-enhanced alleles (ACAGG) showed significantly higher luciferase activities in three different human cell lines (e.g., A375, SK, and KB) than for the other two major haplotypes (Figure 2c–e). When examined individually, the SL-enhanced alleles of the five SNPs showed significant effects on reporter gene expression but in different directions (Figure 2c–e). The SL-enhanced alleles of rs2853672 and rs2736098 upregulated gene transcription, which is consistent with the haplotype effect, whereas rs2853669, rs2735940, and rs7712562 had the opposite effect. This positive correlation between SL-enhanced SNP alleles and *TERT* expression level was also supported by the publicly available expression quantitative trait loci database at GTEx (Supplementary Table S8) (e.g., rs2853672, $\beta = 0.22$, $P = 9.50 \times 10^{-6}$). Furthermore, a two-sample–based Mendelian randomization test indicated that the upregulated *TERT* expression could be a potential causal factor of non-facial SL (Supplementary Figure S3).

To further assess the effect of rs2853672 and rs2736098 on the expression level of *TERT*, we performed CRISPR-Cas9 experiments with single-guide RNAs targeting the genomic regions surrounding these sites or a control single-guide RNA (Figure 2f). By RT-qPCR analysis, we found that the infected cells displayed significantly reduced endogenous *TERT* expression and telomere length compared with the control cells (Figure 2g and h).

Interestingly, the SNPs rs2853672 and rs2736098 are also DNA methylation quantitative trait loci of methylation sites in *TERT* (Gaunt et al., 2016; Heyn et al., 2014), which was confirmed in the NSPT cohort where methylation data are available ($P = 1.66 \times 10^{-241}$) (Figure 3a). We found that one of the DNA methylation quantitative trait loci–related 5′-C-phosphate-G-3′, cg23827991, was also significantly associated with non-facial SL (beta-coefficient = 1.68, $P = 1.45 \times 10^{-8}$) (Figure 3b). Using dual-luciferase reporter assay experiments in two different cell lines (e.g., 293T and A375), we confirmed that hypermethylation at cg23827991 was associated with lower *TERT* transcription levels (Figure 3c and d).

All the results mentioned earlier are consistent with the assumption that the SNPs rs2853672 and rs2736098 affect the expression of *TERT* and that the upregulation of *TERT* is likely to be causally linked to SL.

TERT-related global aging markers were not associated with SL

TERT is well-known to be associated with global aging markers, that is, leukocyte telomere length (LTL) (Bojesen

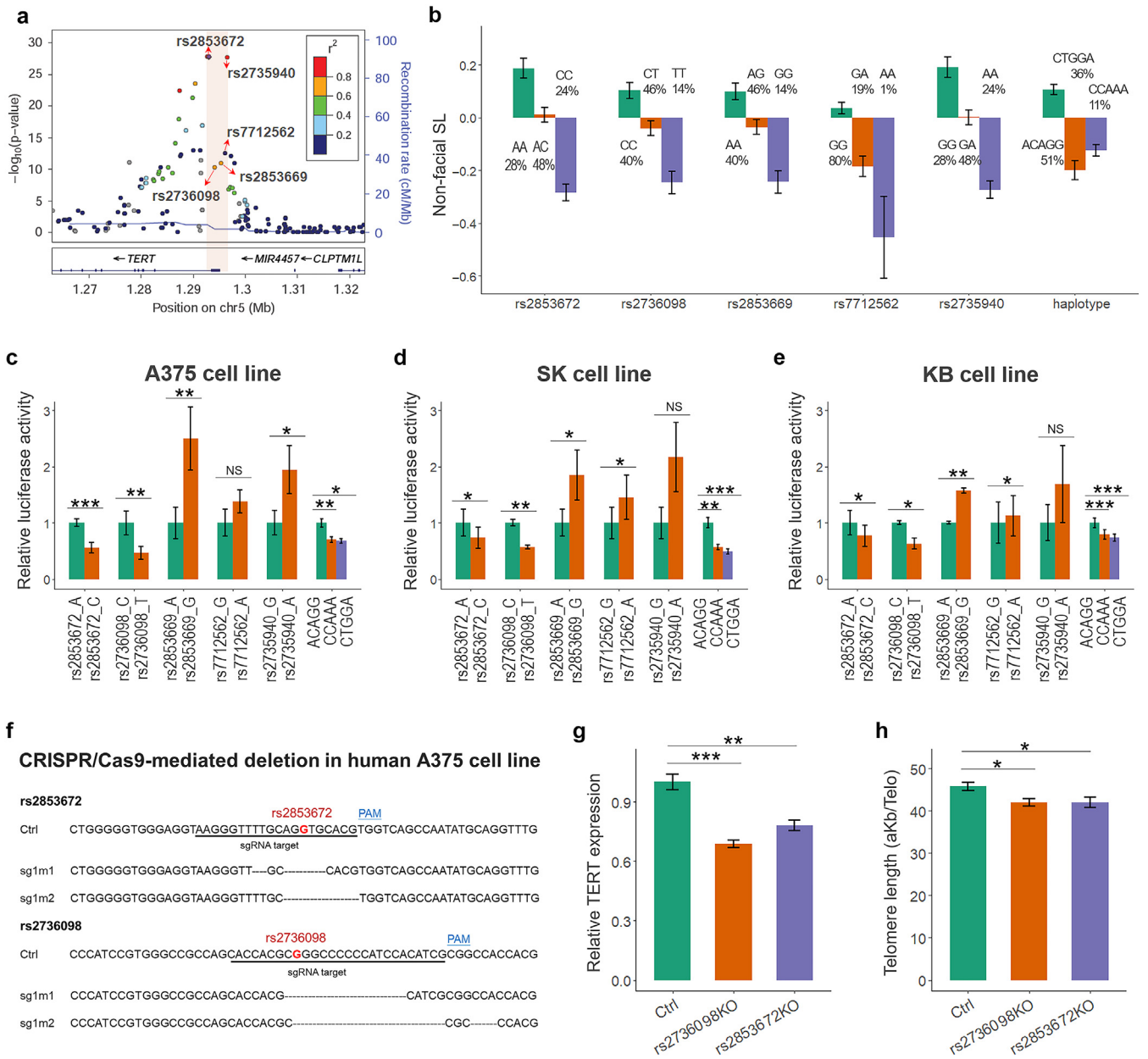

Figure 2. Functional validation of 5p15.33. (**a**) Locuszoom of five potential functional SNPs (red arrows). (**b**) Barplot of non-facial SL according to genotype or haplotype at five SNPs. (**c–e**) Luciferase reporter activity for allele or haplotype of five SNPs in A375, SK, and KB cell lines. (**f**) DNA sequencing results of genomic regions around rs2853672 or rs2736098 sites (red) in Ctrl A375 cells and their corresponding CRISPR-edited clones (672mut and 098mut). sgRNA sequences were underlined. (**g, h**) RT-qPCR analysis of relative *TERT* expression level (left) and telomere length (right) in A375 cells stabling infected with control CRISPR lentivirus (Ctrl) or rs2736098 (098-KO) or rs2853672 (672-KO) site. The bar represents mean ± error. $^{*}P < 0.05$, $^{**}P < 0.01$, $^{***}P < 0.001$. n = 6 each. Ctrl, control; KO, knockout; sgRNA, single-guide RNA; SL, solar lentigines; TERT, telomerase reverse transcriptase.

et al., 2013; Codd et al., 2013; Dorajoo et al., 2019; Li et al., 2020; Pooley et al., 2013) and intrinsic epigenetic age acceleration (IEAA) (Lu et al., 2018; McCartney et al., 2021); skin aging-related traits, that is, seborrhoeic keratosis (Ghoussaini et al., 2021; Mountjoy et al., 2021); and pigmentation-related trait, that is, basal cell carcinoma (Adolphe et al., 2021). We therefore next tested whether the *TERT* signal contributed to SL through these traits. To this end, data were available for LTL in 800 samples in TZL and for IEAA in 2,954 samples in NSPT. We found no significant association between SL and LTL or SL and IEAA (Figure 4a and b). The LTL was found to be associated with age but not with the *TERT* variants, which might be due to the limited power of our study because of the small sample size (n = 800) (Figure 4c and Supplementary Table S9). In contrast, the IEAA was associated with the *TERT* variants ($P = 3.21 \times 10^{-9}$) (Figure 4d). By taking advantage of the publicly available GWAS summary data of LTL and IEAA in large cohorts (Bojesen et al., 2013; Codd et al., 2013; Dorajoo et al., 2019; Li et al., 2020; Lu et al., 2018; McCartney et al., 2021; Pooley et al., 2013), we used two-sample-based Mendelian randomization tests to evaluate the relationship among LTL,

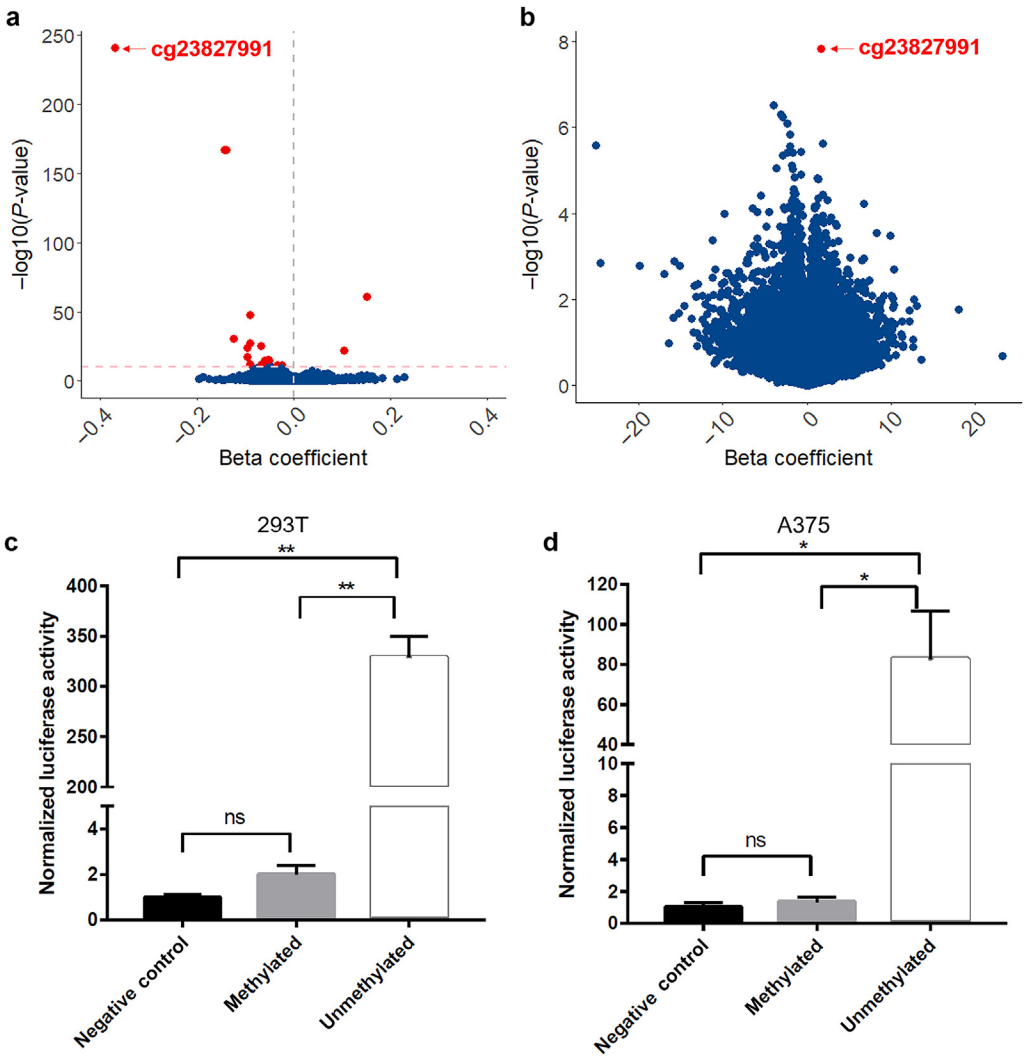

Figure 3. 5p15.33 contribute to non-facial SL through mediation on local DNAm methylation. (**a**) Volcano plot of rs2853672 association with EPIC DNAm sites in NSPT. The red dots indicate significant associations, and the blue dots indicate nonsignificant associations. The red arrow indicates that rs2853672 is significantly associated with cg23827991. (**b**) Volcano plot of association with non-facial SL and EPIC DNAm sites in NSPT. The red dots indicate significant associations, and the blue dots indicate nonsignificant associations. The red arrow indicates that cg23827991 is significantly associated with non-facial SL. (**c, d**) Cellular-based dual-luciferase reporter assay about methylation states of cg23827991 and *TERT* expression in 293T and A375 cell lines. Each bar represents normalized luciferase activity with an error bar in control or different methylation states. $*P < 0.05$ and $**P < 0.01$. n = 2 each. ns, not significant; NSPT, National Survey of Physical Traits; SL, solar lentigines; TERT, telomerase reverse transcriptase.

IEAA, and SL. Although the power was still not enough to support a strong conclusion (Supplementary Table S10), our analysis confirmed the pleiotropic effect between LTL and IEAA ($P_{pleiotropic} = 1.93 \times 10^{-4}$), whereas it did not suggest pleiotropic or causal effects between LTL or IEAA on SL (Supplementary Table S11). We also applied another Mendelian randomization method, CAUSE (Morrison et al., 2020), to explore whether there were sharing or causal relationships between SL and four traits (LTL, IEAA, seborrhoeic keratosis, and basal cell carcinoma). The results implied no sharing or causal relations between SL and these four traits (Supplementary Table S12). Taken together, these results suggest that the effect of *TERT* on SL does not seem to be mediated by LTL, IEAA, seborrhoeic keratosis, or basal cell carcinoma. Nonetheless, these conclusions still need direct validation.

Environmental factors mediate the genetic difference between facial and non-facial SL

In this study, we found that the leading SNP (rs2853672) of the *TERT* signal of non-facial SL ($\beta_{meta} = -0.19$, $P_{meta} = 4.93 \times 10^{-44}$) was only nominally associated with facial SL ($\beta_{meta} = -0.07$, $P_{meta} = 4.42 \times 10^{-7}$) (Supplementary Table S13). A good proportion of candidate genes associated with facial and non-facial SLs also showed quite different significance (Supplementary Table S6). To further explore the reasons behind these varied genetic associations, we compared the phenotypic and genetic correlations between facial and non-facial SLs. The correlation between facial and non-facial SLs was 0.49 (95% confidence interval = 0.47–0.52) in TZL and 0.59 (95% confidence interval = 0.57–0.61) in NSPT, whereas the genetic correlation was $r_g = 1.00$ (Standard error [SE = 0.10]) in TZL and $r_g = 0.96$ (SE = 0.04) in NSPT. This indicates that environmental factors might contribute to the difference in facial and non-facial SLs.

Although several studies disclosed various environmental factors that might affect SL (Ezzedine et al., 2013; Grether-Beck et al., 2021; Hüls et al., 2016; Vierkötter et al., 2010), none of the studies focused on the effect of environmental factors on facial and non-facial SLs. In this study, we explored the effect of various environmental factors (e.g., sun exposure, skin care habit, dietary, education, and social-economic factors) on facial and non-facial SLs. We found that most of these factors have different or opposite effects on facial and non-facial SLs (Supplementary Table S14). For

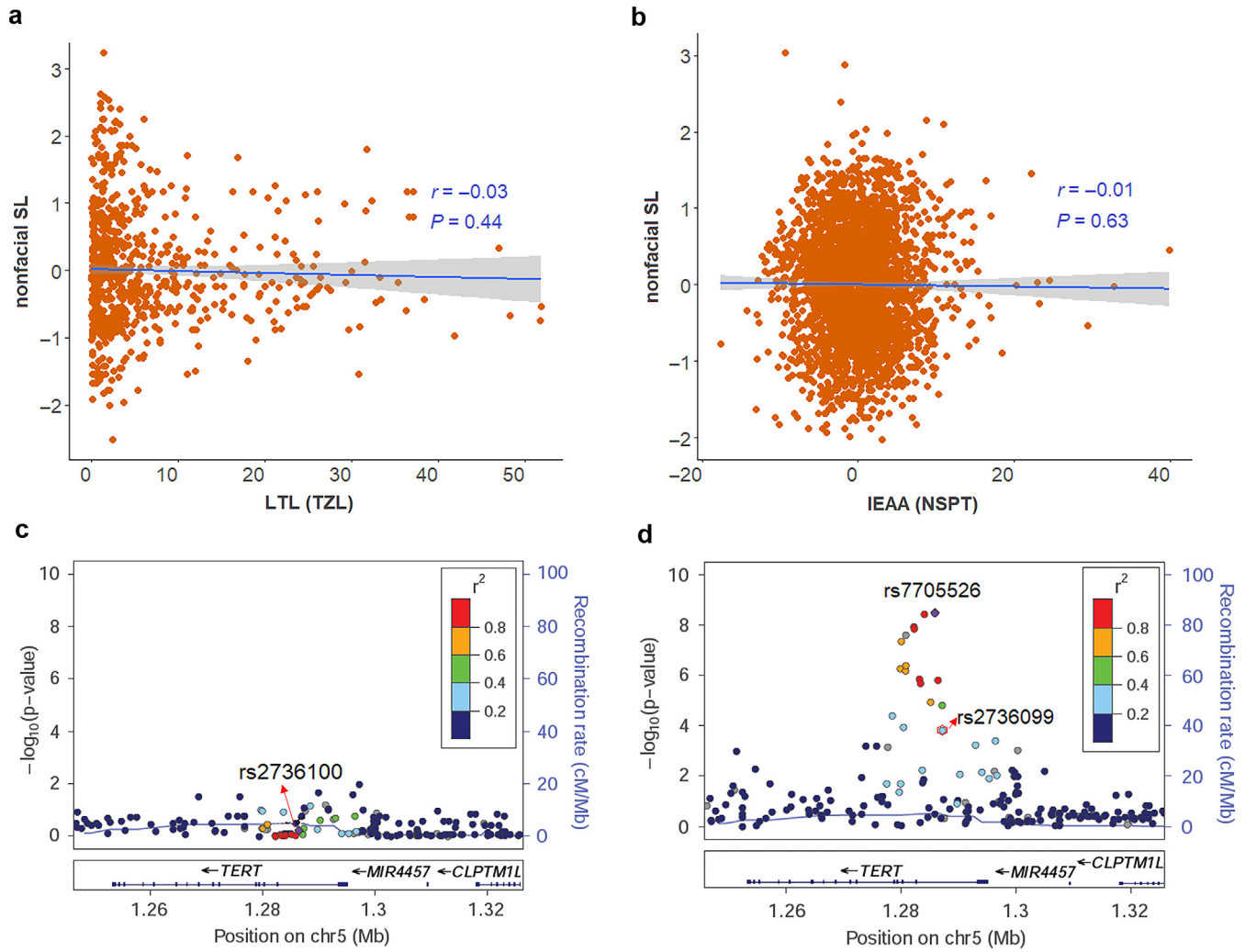

Figure 4. Relationship among 5p15.33 signal, LTL, IEAA, and non-facial SL. (**a**) Scatterplot of LTL and non-facial SL in 800 Han Chinese. (**b**) Scatterplot of IEAA and non-facial SL in NSPT. The blue lines indicate the regression lines of non-facial SL along with LTL or IEAA after adjusting for age. (**c**) Locuszoom of 5p15.33 with LTL in 800 Han Chinese (a subset of TZL). (**d**) Locuszoom of 5p15.33 with IEAA in NSPT. rs2736100 and rs2736099 are the SNPs previously reported to be associated with LTL and IEAA, respectively. rs7705526 is the significant SNV associated with IEAA in NSPT. Pearson correlation (*r*) and *P*-values are also shown in **a** and **b**. IEAA, intrinsic epigenetic age acceleration; LTL, leukocyte telomere length; NSPT, National Survey of Physical Traits; SL, solar lentigines; TERT, telomerase reverse transcriptase; TZL, Taizhou longitudinal cohort.

example, the effect of mean sun exposure time on facial SL is −0.05 (SE = 0.01, $P = 2.90 \times 10^{-5}$), whereas that on non-facial SL is 0.04 (SE = 0.01, $P = 1.95 \times 10^{-5}$). Living in urban versus rural areas contributed significantly to facial SL (beta = −0.46, $P = 4.87 \times 10^{-24}$, $R^2 = 3.72\%$) but less to non-facial SL (beta = 0.1, $P = 0.01$, $R^2 = 0.23\%$).

Previous studies indicated that sun exposure (photoaging) could activate *TERT* expression in exposed skin areas (Attia et al., 2010; Downs et al., 2012). In this study, we separated individuals into high and low sun-exposure groups according to their mean sun exposure time (mean sun exposure time >2 per day or not). We found that the association between *TERT* signal (rs2853672) and non-facial SL was higher in high sun-exposure group than in those in low sun-exposure group (TZL: $\beta_{\text{high exposure}} = -0.26$, $P_{\text{high exposure}} = 2.21 \times 10^{-18}$, $\beta_{\text{low exposure}} = -0.17$, $P_{\text{low exposure}} = 6.18 \times 10^{-6}$; NSPT: $\beta_{\text{high exposure}} = -0.20$, $P_{\text{high exposure}} = 3.20 \times 10^{-13}$, $\beta_{\text{low exposure}} = -0.12$, $P_{\text{low exposure}} = 6.77 \times 10^{-7}$) (Supplementary Table S15). The association between rs2853672 and facial SL indicated similar conclusions (TZL: $\beta_{\text{high exposure}} = -0.10$, $P_{\text{high exposure}} = 0.001$, $\beta_{\text{low exposure}} = -0.06$, $P_{\text{low exposure}} = 0.13$; NSPT: $\beta_{\text{high exposure}} = -0.08$, $P_{\text{high exposure}} = 8.60 \times 10^{-4}$, $\beta_{\text{low exposure}} = -0.02$, $P_{\text{low exposure}} = 0.29$). These findings suggest that sun exposure might mediate the relation between *TERT* and SL.

DISCUSSION

In this study, we provide genetic evidence for an unexpected and previously unrecognized role of *TERT* in the development of SL. Accordingly, through *trans*-ethnic GWASs and meta-studies, we discovered that genetic variants in *TERT* were significantly associated with non-facial SL. These variants were likely of functional relevance for *TERT* expression because SL-enhanced alleles/haplotypes tended to upregulate *TERT* transcription in vitro. Various studies in human and animal models have been conducted to disclose mechanisms underlying the formation of SL (Aoki and Moro, 2005; Aoki

et al., 2007; Barysch et al., 2019; Chen et al., 2010; Endo et al., 2018; Ezzedine et al., 2013; Gao et al., 2017; Hafner et al., 2009; Hasegawa et al., 2015; Jacobs et al., 2015; Kovacs et al., 2010; Laville et al., 2016; Lin et al., 2010; Liu et al., 2019; Motokawa et al., 2008, 2007; Shin et al., 2021; Vierkötter et al., 2012; Yamada et al., 2019). However, in none of these studies had the role of *TERT* in SL been noted.

Of note, GWASs also found significant associations of *TERT* with a large range of other traits, for example, LTL, IEAA, seborrhoeic keratosis, and basal cell carcinoma (Adolphe et al., 2021; Dorajoo et al., 2019; Ghoussaini et al., 2021; Li et al., 2020; McCartney et al., 2021; Mountjoy et al., 2021). In our study, we find that the *TERT* locus is unlikely to modulate the risk of SL through its impact on these traits. However, these conclusions need to be further validated because they come from Mendelian randomization tests, which might be biased from several aspects, for example, confounders of the exposure–outcome association, weak instruments, and sample difference. The mechanism from *TERT* SNPs to SL should be explored in further studies.

In this study, we showed that facial and non-facial SL share similar genetic factors. Genetic correlation between facial and non-facial SLs indicated a largely shared genetic basis between them, although the accuracy of this estimation may be affected by the relatively small sample size in our study. Most genes reported to be associated with facial SL were also associated with non-facial SL and facial SL in our study. In addition, the GWAS signal of non-facial SL in *TERT* was also nominally associated with facial SL in Han Chinese, Caucasian, and Korean (Shin et al., 2021) populations, with effect in the same direction. Although there are histopathological differences between facial and non-facial SLs (Barysch et al., 2019), non-facial SL and facial SL do not seem to be genetically different.

Through *trans*-ethnic GWASs and meta-studies, we discovered that genetic variants in *TERT* were significantly associated with non-facial SL. The heterogeneity measures of *TERT* SNPs (rs2853672, $I^2 = 77.2$, $Q = 8.77$, $P_{HET} = 0.01$ for nonfacial SL, $I^2 = 67.9$, $Q = 6.22$, $P_{HET} = 0.04$ for facial SL) (Supplementary Table S16) indicate substantial heterogeneity. We could rule out the possibility that population or phenotyping differences were causing the heterogeneity because the minor allele frequencies of *TERT* SNP, for example, rs2853672, is around 0.5 in TZL, NSPT, and SALIA, and the same phenotypes were applied in each study. The heterogeneity might originate from sampling bias, especially in the quite small German cohort. It also has to be noted that the heterogeneity measure itself would be biased owing to the fact that there were only three studies included in the meta-analysis.

However, our results suggest that the power to detect genetic variants in *TERT* associated with facial SL is lower than that associated with non-facial SL. In fact, we believe that various confounding factors may interfere with such genetic association analysis. As discussed in previous studies (Jacobs et al., 2015), the phenotyping of facial SLs might have been confounded by other pigmented, maculous lesions that frequently occur in the face but are absent in non-facial skin areas. In addition, most humans regularly use cosmetic daycare products on their faces but much less frequently in non-facial skin sites. The vast majority of facial daycare products contain UV filters (Ezzedine et al., 2013), and their regular use is likely to significantly reduce the clinical signs of photoaging of human skin such as SL (Hasegawa et al., 2015). We found that frequent skin care was significantly and negatively associated with facial SL but did not associate with non-facial SL at all. Besides, there are factors beyond UV exposure that contribute to different extents of facial versus non-facial SL (Nakamura et al., 2015). In our study, we found that mean sun exposure time, skin care habits, dietary, education, and social-economic factors had different or opposite effects on facial versus non-facial SL**.** The substantially higher genetic correlation than phenotypic correlation between facial and non-facial SL may be explained by the distinctive contributions of nongenetic (environmental) factors to facial and non-facial SL.

The promoter region of the *TERT* gene is considered the most important regulatory element for telomerase expression. It spans 330 base pair upstream of the translational start site and 37 base pair of exon 2 and is known to be enriched with transcriptional-binding sites/consensus sites that interact with both negative and positive regulators of *TERT* (Pestana et al., 2017). In this study, we assessed the functional role of rs2853672 and rs2736098 for regulating *TERT* transcription by four strategies: (i) allele/haplotype-based luciferase reporter assays in three human cell lines, (ii) Cas9 gene editing experiments, (iii) analysis of reported expression quantitative trait loci (GTEx, https://gtexportal.org/), and (iv) DNA methylation quantitative trait loci and luciferase reporter assays. All of the obtained results are consistent with the conclusion that the SNPs rs2853672 and rs2736098 affect the expression of *TERT* and that the upregulation of *TERT* expression is causally linked to SL.

Previous study has shown that only in the skin exposed to a high amount of UV rays, *WNT1* expression upregulated and promoted melanocytogenesis and melanogenesis in SL skin (Yamada et al., 2019). The increased expression of *TERT* was also found in the skin during sun exposure (Attia et al., 2010; Downs et al., 2012). In this study, we discovered that the association between *TERT* SNPs and SL was higher in the high sun-exposure group than in low sun-exposure group, which confirmed that genotoxicity (UV exposure) might mediate the relation between *TERT* and SL.

The results of this study indicate that *TERT* plays a previously unrecognized role in the pathogenesis of SL. The exact nature of the mechanisms that are affected by *TERT* in this context is currently not known. There is evidence that *TERT* can promote the survival and proliferation of melanoma cells (Pestana et al., 2017; Seynnaeve et al., 2017; Yuan et al., 2019). It has also been suggested that *TERT* is involved in several key signaling pathways in melanocytes and keratinocytes, such as Wnt/β-catenin, NF-kB, and protein kinase B/mTOR signaling pathway (Ali et al., 2016; Ghareghomi et al., 2021; Hirobe et al., 2002; Yamada et al., 2014). Whether and to what extent the effect of *TERT* on these or other mechanisms might contribute to the development of SL will have to be assessed in further studies, which are beyond the scope of the present genetic analysis.

MATERIALS AND METHODS

Population and samples

The first discovery panel included 2,964 Han Chinese individuals (TZL, 1,059 males and 1,905 females with ages ranging from 31 to 86 years, mean ± SD = 55.9 ± 9.4) recruited in Taizhou in Jiangsu Province in 2014 (Wang et al., 2009). Questionnaire responses (including sex, age, and other information) and blood samples were collected from each individual. The second included 2,954 Han Chinese samples collected in three regional districts (Taizhou, Nanning, and Zhengzhou) of China (NSPT, 1,109 males and 1,845 females, aged from 19 to 83 years, mean ± SD = 49.7 ± 13.2) from 2015 to 2019. The replication data included 462 Caucasian females aged 66.7–79.4 years sampled from the SALIA cohort in Germany (Schnass et al., 2018). A detailed description of the SALIA study has been previously provided by Schikowski et al. (2005). The research was conducted with the official written approval (written form) of the Ethics Committee of Fudan University (Shanghai, China). All the participants in Han Chinese samples provided written informed consent. All participants in SALIA gave written informed consent, and the Medical Ethics Committee of the University of Bochum approved the follow-up examination.

Evaluation of pigmented spots on hands/arms

We collected SL on the face and hands/arms according to the SCINEXA method (score of intrinsic and extrinsic skin aging [Vierkötter et al., 2009]); for more information, see Supplementary Materials and Methods.

Extract composite phenotype

In the discovery cohort (TZL), the correlation among the seven SL traits appeared to be two clusters, one comprising three non-facial SL traits, whereas the other comprising four facial SL traits (Supplementary Figure S2a and Supplementary Table S1). Then, we applied PLSPM to extract two composite phenotypes from three non-facial SL and four facial SL traits and denoted them as composite phenotypes of non-facial and facial SLs. The outer model in PLSPM was constructed on the basis of structures learned from correlation analysis (Supplementary Figure S2b), and for the inner model, it comprised, by age, composite phenotypes of facial SL and non-facial SLs. The reflective model was applied in PLSPM, and the bootstrap method was used to estimate all the parameters in the model. The model fitted well, with the internal homogeneity of each composite phenotype being much higher than that of external ones. Finally, we extracted the composite phenotypes of facial and non-facial SLs from the PLSPM scores and took them as the studied phenotypes in this study. The same PLSPM model was applied to obtain the composite phenotypes of facial and non-facial SLs in the other two cohorts (NSPT and SALIA). This work was done using the R package PLSPM.

Genotyping

Genomic DNA was extracted from blood samples using the MagPure Blood DNA KF Kit (MGBio, Shanghai, China). Genotyping of 2,964 Han Chinese samples (TZL) was done using the Illumina Human OmniZhonghua8, version 1.1 895k (Illumina, San Diego, CA). Genotyping of 2,954 samples (NSPT) was performed using the Illumina Infinium Global Screening Array (Illumina). Genotyping of 462 German samples (SALIA) was performed using Affymetrix Axiom Precision Medicine Research Array (Affymetrix, Santa Clara, CA) (for more information, see Supplementary Materials and Methods).

DNA methylation

The methylation data of 2,954 Han Chinese in NSPT were generated using Illumina Methylation EPIC850 K (Illumina) (for more information, see Supplementary Materials and Methods).

Statistical analysis

Heritability estimation. Heritability analysis was conducted using GREML-LDMS (the linkage disequilibrium and minor allele frequency stratified [LDMS] genetic restricted maximum likelihood [GREML] approach) [Yang et al., 2015]) in TZL and NSPT after removing the related samples to ensure that all the samples have identity by descent (IBD) smaller than 0.05. Variants were stratified into two MAF bins (MAF $<$ 0.01 and MAF $\geq$ 0.01) as well as two linkage disequilibrium groups above or below the median regional linkage disequilibrium score. The genetic relationship matrix from each MAF–linkage disequilibrium stratum was calculated and fitted jointly in a mixed linear model.

GWAS. All GWASs were conducted by Genome-wide Complex Trait Analysis (fastGWA) (Jiang et al., 2019), which could adjust relatedness in the model. GWASs were performed by a linear regression and additive model adjusted for age, sex, and top 10 principal components. Skin color was also adjusted in a subset-based GWAS in TZL. Bonferroni correction ($P < 5 \times 10^{-8}$) was applied to all GWAS results.

Conditional GWAS. Conditional analysis on the leading SNP (rs2853672) was also performed using –cojo-cond option implemented in Genome-wide Complex Trait Analysis (fastGWA) (Jiang et al., 2019). The model is applied by a linear regression of additive model adjusted for age, sex, and top 10 principal components and conditioned on top SNP rs2853672 in TZL. The *P*-value of association tests was adjusted by Bonferroni correction ($P < 5 \times 10^{-8}$).

Meta-analysis. The fixed-effect meta-analyses were performed on the cleaned files using METAL (Willer et al., 2010), with the Effective N as weight. Meta-analysis was applied to the two Han Chinese cohorts (TZL and NSPT) and also to three cohorts (TZL, NSPT, and SALIA). Bonferroni correction ($P < 5 \times 10^{-8}$) was applied to all meta-results.

Replication of previous GWAS signals. The replication results of previous GWAS signals were extracted from the meta-results of two Han Chinese cohorts. No correction of *P*-values was conducted.

Haplotype analysis. Haplotype phasing, frequency estimation, and association analysis of five SNPs (rs2853672, rs2736098, rs2853669, rs2735940, and rs7712562) were performed in the R package haplo.stats.

Other methods applied in this study are incorporated in Supplementary Materials and Methods.

Code availability

Most operations were carried out by R (https://cran.r-project.org/), and the plots were mainly made by the ggplot2 R package (https://cran.r-project.org/web/packages/ggplot2/index.html). The two-sample Mendelian randomization analysis was conducted using the TwoSampleMR R package (https://mrcieu.github.io/TwoSampleMR/). GWASs were carried out by PLINK (http://pngu.mgh.harvard.edu/~purcell/plink/). SNP heritability was calculated using Genome-wide Complex Trait Analysis (https://yanglab.westlake.edu.cn/software/gcta/#Overview).

Meta-analysis was carried out by Metal (http://www.sph.umich.edu/csg/abecasis/metal/).

Data availability statement

The summary statistics of facial and non-facial solar lentigines GWAS in three cohorts (Taizhou longitudinal cohort, National Survey of Physical Traits, and SALIA) can be viewed at NODE (https://www.biosino.org/node) under accession number OEZ008165 or directly at https://www.biosino.org/node/analysis/detail/OEZ008165 and accessed by submitting a request for data access. The SNP chip data in the Taizhou longitudinal cohort and National Survey of Physical Traits are accessed by submitting a request for data access. Data usage shall be in full compliance with the Regulations on Management of Human Genetic Resources in China. The SNP chip data in SALIA are only available by submitting data requests to jean.krutmann@iuf-duesseldorf.de. All other relevant data supporting the key findings of this study are available within the article and its supplementary files or from the corresponding author upon reasonable request. The expression quantitative trait loci results in whole blood were downloaded from GTEx (https://www.gtexportal.org/home/datasets), including RNA-sequencing data Transcript TPMs (dbGaP accession number phs000424.v8.p2 on 06/05/2017) and tissue-specific All SNP Gene Associations (dbGaP accession number phs000424.v7.p2 on 01/15/2016).

ORCIDs

Qianqian Peng: http://www.orcid.org/0000-0002-2018-5706
Yu Liu: http://www.orcid.org/0000-0001-7110-127X
Anke Huels: http://www.orcid.org/0000-0002-6005-417X
Canfeng Zhang: http://www.orcid.org/0000-0002-8480-5097
Yao Yu: http://www.orcid.org/0000-0003-2849-1342
Wenqing Qiu: http://www.orcid.org/0000-0002-6245-197X
Xiyang Cai: http://www.orcid.org/0000-0002-3868-5426
Yuepu Zhao: http://www.orcid.org/0000-0002-4179-7533
Tamara Schikowski: http://www.orcid.org/0000-0002-4559-9374
Katja Merches: http://www.orcid.org/0000-0002-3411-8686
Yun Liu: http://www.orcid.org/0000-0001-5753-1265
Yajun Yang: http://www.orcid.org/0000-0001-5713-0103
Jiucun Wang: http://www.orcid.org/0000-0003-2765-0620
Yong Zhao: http://www.orcid.org/0000-0001-5068-2212
Li Jin: http://www.orcid.org/0000-0001-9201-2321
Liang Zhang: http://www.orcid.org/0000-0003-4396-9199
Jean Krutmann: http://www.orcid.org/0000-0001-8433-1517
Sijia Wang: http://www.orcid.org/0000-0001-6961-7867

CONFLICT OF INTEREST

The authors state no conflict of interest.

ACKNOWLEDGMENT

The authors acknowledge the following funding sources: the Strategic Priority Research Program of the Chinese Academy of Sciences (grant numbers XDB38020400 and XDA160101XX), the National Key Research and Development Project (grant numbers 2017YFA0103500 and 2017YFA0102800), the National Natural Science Foundation of China (grant numbers 92249302, 32070730, 31471385, and 81673104), Shanghai Municipal Science and Technology Major Project (grant numbers 2017SHZDZX01 and 21JC1406400), CAS Interdisciplinary Innovation Team, CAS Project for Young Scientists in Basic Research (grant number YSBR-077), CAS Youth Innovation Promotion Association (grant number 2020276), and Innovative research team of high-level local universities in Shanghai. YGZ is deceased.

AUTHOR CONTRIBUTIONS

Conceptualization: SW, JK; Data Curation: QP, YL, XC, YPZ, AH, TS, KM; Formal Analysis: QP, YL, CZ, YY, WQ; Funding Acquisition: SW, JK, YGZ, LZ, YL, QP; Investigation: QP, YL, AH, TS, KM; Methodology: QP, YL; Project Administration: SW, JK; Resources: SW, JK, LJ, YJY, JW; Supervision: SW, JK; Validation: AH, TS, KM, JK, LJ, YJY, JW; Visualization: QP, YL, CZ, YY, WQ; Writing – Original Draft Preparation: QP, YL; Writing – Review and Editing: SW, JK, QP, YL

SUPPLEMENTARY MATERIAL

Supplementary material is linked to the online version of the paper at www.jidonline.org, and at https://doi.org/10.1016/j.jid.2022.11.016.

REFERENCES

Adhikari K, Mendoza-Revilla J, Sohail A, Fuentes-Guajardo M, Lampert J, Chacón-Duque JC, et al. A GWAS in Latin Americans highlights the convergent evolution of lighter skin pigmentation in Eurasia. Nat Commun 2019;10:358.

Adolphe C, Xue A, Fard AT, Genovesi LA, Yang J, Wainwright BJ. Genetic and functional interaction network analysis reveals global enrichment of regulatory T cell genes influencing basal cell carcinoma susceptibility. Genome Med 2021;13:19.

Ali M, Devkota S, Roh JI, Lee J, Lee HW. Telomerase reverse transcriptase induces basal and amino acid starvation-induced autophagy through mTORC1. Biochem Biophys Res Commun 2016;478:1198–204.

Aoki H, Moro O. Upregulation of the IFN-gamma-stimulated genes in the development of delayed pigmented spots on the dorsal skin of F1 mice of HR-1 x HR/De. J Invest Dermatol 2005;124:1053–61.

Aoki H, Moro O, Tagami H, Kishimoto J. Gene expression profiling analysis of solar lentigo in relation to immunohistochemical characteristics. Br J Dermatol 2007;156:1214–23.

Attia EA, Seada LS, El-Sayed MH, El-Shiemy SM. Study of telomerase reverse transcriptase (hTERT) expression in normal, aged, and photo-aged skin. Int J Dermatol 2010;49:886–93.

Barysch MJ, Braun RP, Kolm I, Ahlgrimm-Siesz V, Hofmann-Wellenhof R, Duval C, et al. Keratinocytic malfunction as a trigger for the development of solar lentigines. Dermatopathology (Basel) 2019;6:1–11.

Bojesen SE, Pooley KA, Johnatty SE, Beesley J, Michailidou K, Tyrer JP, et al. Multiple independent variants at the tert locus are associated with telomere length and risks of breast and ovarian cancer. Nat Genet 2013;45:371–84. 84.e1–2.

Chen N, Hu Y, Li WH, Eisinger M, Seiberg M, Lin CB. The role of keratinocyte growth factor in melanogenesis: a possible mechanism for the initiation of solar lentigines. Exp Dermatol 2010;19:865–72.

Codd V, Nelson CP, Albrecht E, Mangino M, Deelen J, Buxton JL, et al. Identification of seven loci affecting mean telomere length and their association with disease. Nat Genet 2013;45(422–7):427e1–2.

Dorajoo R, Chang X, Gurung RL, Li Z, Wang L, Wang R, et al. Loci for human leukocyte telomere length in the Singaporean Chinese population and trans-ethnic genetic studies. Nat Commun 2019;10:2491.

Downs KP, Shen Y, Pasquali A, Beldorth I, Savage M, Gallier K, et al. Characterization of telomeres and telomerase expression in Xiphophorus. Comp Biochem Physiol C Toxicol Pharmacol 2012;155:89–94.

Eaton K, Edwards M, Krithika S, Cook G, Norton H, Parra EJ. Association study confirms the role of two OCA2 polymorphisms in normal skin pigmentation variation in East Asian populations. Am J Hum Biol 2015;27:520–5.

Edwards M, Bigham A, Tan J, Li S, Gozdzik A, Ross K, et al. Association of the OCA2 polymorphism His615Arg with melanin content in east Asian populations: further evidence of convergent evolution of skin pigmentation. PLoS Genet 2010;6:e1000867.

Endo C, Johnson TA, Morino R, Nakazono K, Kamitsuji S, Akita M, et al. Genome-wide association study in Japanese females identifies fifteen novel skin-related trait associations. Sci Rep 2018;8:8974.

Ezzedine K, Mauger E, Latreille J, Jdid R, Malvy D, Gruber F, et al. Freckles and solar lentigines have different risk factors in Caucasian women. J Eur Acad Dermatol Venereol 2013;27:e345–56.

Feng Y, McQuillan MA, Tishkoff SA. Evolutionary genetics of skin pigmentation in African populations. Hum Mol Genet 2021;30:R88–97.

Gao W, Tan J, Hüls A, Ding A, Liu Y, Matsui MS, et al. Genetic variants associated with skin aging in the Chinese Han population. J Dermatol Sci 2017;86:21–9.

Gaunt TR, Shihab HA, Hemani G, Min JL, Woodward G, Lyttleton O, et al. Systematic identification of genetic influences on methylation across the human life course. Genome Biol 2016;17:61.

Ghareghomi S, Ahmadian S, Zarghami N, Kahroba H. Fundamental insights into the interaction between telomerase/tert and intracellular signaling pathways. Biochimie 2021;181:12–24.

Ghoussaini M, Mountjoy E, Carmona M, Peat G, Schmidt EM, Hercules A, et al. Open Targets Genetics: systematic identification of trait-associated

genes using large-scale genetics and functional genomics. Nucleic Acids Res 2021;49:D1311–20.

Grether-Beck S, Felsner I, Brenden H, Marini A, Jaenicke T, Aue N, et al. Air pollution-induced tanning of human skin. Br J Dermatol 2021;185:1026–34.

Gunn DA, Rexbye H, Griffiths CE, Murray PG, Fereday A, Catt SD, et al. Why some women look young for their age. PLoS One 2009;4:e8021.

Hafner C, Stoehr R, van Oers JM, Zwarthoff EC, Hofstaedter F, Landthaler M, et al. FGFR3 and PIK3CA mutations are involved in the molecular pathogenesis of solar lentigo. Br J Dermatol 2009;160:546–51.

Hasegawa K, Fujiwara R, Sato K, Shin J, Kim SJ, Kim M, et al. Possible involvement of keratinocyte growth factor in the persistence of hyperpigmentation in both human facial solar lentigines and Melasma. Ann Dermatol 2015;27:626–9.

Helbig S, Wockner L, Bouendeu A, Hille-Betz U, McCue K, French JD, et al. Functional dissection of breast cancer risk-associated tert promoter variants. Oncotarget 2017;8:67203–17.

Heyn H, Sayols S, Moutinho C, Vidal E, Sanchez-Mut JV, Stefansson OA, et al. Linkage of DNA methylation quantitative trait loci to human cancer risk. Cell Rep 2014;7:331–8.

Hirobe T, Furuya R, Akiu S, Ifuku O, Fukuda M. Keratinocytes control the proliferation and differentiation of cultured epidermal melanocytes from ultraviolet radiation B-induced pigmented spots in the dorsal skin of hairless mice. Pigment Cell Res 2002;15:391–9.

Hüls A, Vierkötter A, Gao W, Krämer U, Yang Y, Ding A, et al. Traffic-related air pollution contributes to development of facial lentigines: further epidemiological evidence from Caucasians and Asians. J Invest Dermatol 2016;136:1053–6.

Jacobs LC, Hamer MA, Gunn DA, Deelen J, Lall JS, van Heemst D, et al. A genome-wide association study identifies the skin color genes IRF4, MC1R, ASIP, and BNC2 influencing facial pigmented spots. J Invest Dermatol 2015;135:1735–42.

Jiang L, Zheng Z, Qi T, Kemper KE, Wray NR, Visscher PM, et al. A resource-efficient tool for mixed model association analysis of large-scale data. Nat Genet 2019;51:1749–55.

Jonnalagadda M, Bharti N, Kasibhatla SM, Wagh MA, Joshi R, Ozarkar S, et al. MC1R diversity and its role in skin pigmentation variation in West Maharashtra, India. Am J Hum Biol 2022;34:e23734.

Ju D, Mathieson I. The evolution of skin pigmentation-associated variation in West Eurasia. Proc Natl Acad Sci USA 2021:118.

Kichaev G, Yang WY, Lindstrom S, Hormozdiari F, Eskin E, Price AL, et al. Integrating functional data to prioritize causal variants in statistical fine-mapping studies. PLoS Genet 2014;10:e1004722.

Ko E, Seo HW, Jung ES, Kim BH, Jung G. The tert promoter SNP rs2853669 decreases E2F1 transcription factor binding and increases mortality and recurrence risks in liver cancer. Oncotarget 2016;7:684–99.

Kovacs D, Cardinali G, Aspite N, Cota C, Luzi F, Bellei B, et al. Role of fibroblast-derived growth factors in regulating hyperpigmentation of solar lentigo. Br J Dermatol 2010;163:1020–7.

Laville V, Clerc SL, Ezzedine K, Jdid R, Taing L, Labib T, et al. A genome-wide association study in Caucasian women suggests the involvement of HLA genes in the severity of facial solar lentigines. Pigment Cell Melanoma Res 2016;29:550–8.

Li C, Stoma S, Lotta LA, Warner S, Albrecht E, Allione A, et al. Genome-wide association analysis in humans links nucleotide metabolism to leukocyte telomere length. Am J Hum Genet 2020;106:389–404.

Lin CB, Hu Y, Rossetti D, Chen N, David C, Slominski A, et al. Immunohistochemical evaluation of solar lentigines: the association of KGF/KGFR and other factors with lesion development. J Dermatol Sci 2010;59:91–7.

Liu Y, Gao W, Koellmann C, Le Clerc S, Hüls A, Li B, et al. Genome-wide scan identified genetic variants associated with skin aging in a Chinese female population. J Dermatol Sci 2019;96:42–9.

Lu AT, Xue L, Salfati EL, Chen BH, Ferrucci L, Levy D, et al. GWAS of epigenetic aging rates in blood reveals a critical role for tert. Nat Commun 2018;9:387.

Ma R, Liu C, Lu M, Yuan X, Cheng G, Kong F, et al. The tert locus genotypes of rs2736100-CC/CA and rs2736098-AA predict shorter survival in renal cell carcinoma. Urol Oncol 2019;37:301.e1–10.

McCartney DL, Min JL, Richmond RC, Lu AT, Sobczyk MK, Davies G, et al. Genome-wide association studies identify 137 genetic loci for DNA methylation biomarkers of aging. Genome Biol 2021;22:194.

Morrison J, Knoblauch N, Marcus JH, Stephens M, He X. Mendelian randomization accounting for correlated and uncorrelated pleiotropic effects using genome-wide summary statistics. Nat Genet 2020;52:740–7.

Motokawa T, Kato T, Hashimoto Y, Katagiri T. Effect of Val92Met and Arg163Gln variants of the MC1R gene on freckles and solar lentigines in Japanese. Pigment Cell Res 2007;20:140–3.

Motokawa T, Kato T, Hashimoto Y, Takimoto H, Yamamoto H, Katagiri T. Polymorphism patterns in the promoter region of the MC1R gene are associated with development of freckles and solar lentigines. J Invest Dermatol 2008;128:1588–91.

Mountjoy E, Schmidt EM, Carmona M, Schwartzentruber J, Peat G, Miranda A, et al. An open approach to systematically prioritize causal variants and genes at all published human GWAS trait-associated loci. Nat Genet 2021;53:1527–33.

Murray N, Norton HL, Parra EJ. Distribution of two OCA2 polymorphisms associated with pigmentation in East-Asian populations. Hum Genome Var 2015;2:15058.

Nakamura M, Morita A, Seité S, Haarmann-Stemmann T, Grether-Beck S, Krutmann J. Environment-induced lentigines: formation of solar lentigines beyond ultraviolet radiation. Exp Dermatol 2015;24:407–11.

Pestana A, Vinagre J, Sobrinho-Simões M, Soares P. Tert biology and function in cancer: beyond immortalisation. J Mol Endocrinol 2017;58:R129–46.

Pooley KA, Bojesen SE, Weischer M, Nielsen SF, Thompson D, Amin Al Olama A, et al. A genome-wide association scan (GWAS) for mean telomere length within the COGS project: identified loci show little association with hormone-related cancer risk. Hum Mol Genet 2013;22:5056–64.

Rawofi L, Edwards M, Krithika S, Le P, Cha D, Yang Z, et al. Genome-wide association study of pigmentary traits (skin and iris color) in individuals of East Asian ancestry. PeerJ 2017;5:e3951.

Rocha J. The evolutionary history of human skin pigmentation. J Mol Evol 2020;88:77–87.

Schikowski T, Sugiri D, Ranft U, Gehring U, Heinrich J, Wichmann HE, et al. Long-term air pollution exposure and living close to busy roads are associated with COPD in women. Respir Res 2005;6:152.

Schnass W, Hüls A, Vierkötter A, Krämer U, Krutmann J, Schikowski T. Traffic-related air pollution and eczema in the elderly: findings from the SALIA cohort. Int J Hyg Environ Health 2018;221:861–7.

Seynnaeve B, Lee S, Borah S, Park Y, Pappo A, Kirkwood JM, et al. Genetic and epigenetic alterations of tert are associated with inferior outcome in adolescent and young adult patients with melanoma. Sci Rep 2017;7:45704.

Sheng X, Tong N, Tao G, Luo D, Wang M, Fang Y, et al. Tert polymorphisms modify the risk of acute lymphoblastic leukemia in Chinese children. Carcinogenesis 2013;34:228–35.

Shin JG, Leem S, Kim B, Kim Y, Lee SG, Song HJ, et al. GWAS analysis of 17,019 Korean women identifies the variants associated with facial pigmented spots. J Invest Dermatol 2021;141:555–62.

Vierkötter A, Krämer U, Sugiri D, Morita A, Yamamoto A, Kaneko N, et al. Development of lentigines in German and Japanese women correlates with variants in the SLC45A2 gene. J Invest Dermatol 2012;132:733–6.

Vierkötter A, Ranft U, Krämer U, Sugiri D, Reimann V, Krutmann J. The SCINEXA: a novel, validated score to simultaneously assess and differentiate between intrinsic and extrinsic skin ageing. J Dermatol Sci 2009;53:207–11.

Vierkötter A, Schikowski T, Ranft U, Sugiri D, Matsui M, Krämer U, et al. Airborne particle exposure and extrinsic skin aging. J Invest Dermatol 2010;130:2719–26.

Wang J, Dayem Ullah AZ, Chelala C, IW-Scoring. an Integrative Weighted Scoring framework for annotating and prioritizing genetic variations in the noncoding genome. Nucleic Acids Res 2018;46:e47.

Wang X, Lu M, Qian J, Yang Y, Li S, Lu D, et al. Rationales, design and recruitment of the Taizhou Longitudinal Study. BMC Public Health 2009;9:223.

Willer CJ, Li Y, Abecasis GR. METAL: fast and efficient meta-analysis of genomewide association scans. Bioinformatics 2010;26:2190–1.

Yamada T, Hasegawa S, Inoue Y, Date Y, Arima M, Yagami A, et al. Accelerated differentiation of melanocyte stem cells contributes to the formation of hyperpigmented maculae. Exp Dermatol 2014;23:652–8.

Yamada T, Hasegawa S, Iwata Y, Arima M, Kobayashi T, Numata S, et al. UV irradiation-induced DNA hypomethylation around WNT1 gene: implications for solar lentigines. Exp Dermatol 2019;28:723–9.

Yang J, Bakshi A, Zhu Z, Hemani G, Vinkhuyzen AA, Lee SH, et al. Genetic variance estimation with imputed variants finds negligible missing heritability for human height and body mass index. Nat Genet 2015;47:1114–20.

Yang Z, Shi H, Ma P, Zhao S, Kong Q, Bian T, et al. Darwinian positive selection on the pleiotropic effects of KITLG explain skin pigmentation and winter temperature adaptation in eurasians. Mol Biol Evol 2018;35:2272–83.

Yang Z, Zhong H, Chen J, Zhang X, Zhang H, Luo X, et al. A genetic mechanism for convergent skin lightening during recent human evolution. Mol Biol Evol 2016;33:1177–87.

Yuan X, Larsson C, Xu D. Mechanisms underlying the activation of tert transcription and telomerase activity in human cancer: old actors and new players. Oncogene 2019;38:6172–83.

SUPPLEMENTARY MATERIALS AND METHODS

The SCINEXA method

The SCINEXA method is a well-established, validated scoring that has been used successfully in a number of previous studies to assess skin aging in Caucasians and Han Chinese (Fuks et al., 2019; Gao et al., 2017; Li et al., 2015; Liu et al., 2019; Vierkötter et al., 2016, 2010, 2009). Skin aging phenotypes that are assessed by SCINEXA include the number of solar lentigines (SL) on the dorsal side of the forearm, the number of SL on the back of hands, uneven pigmentation on the ventral side of forearms, the size and number of SL on the forehead, and the size and number of SL on cheeks. A detailed description of the evaluation methods of each of these phenotypes is shown in Supplementary Figure S1. The severity of SL on both sides of the forearm and back of the hands was evaluated separately (Supplementary Figure S1). The phenotypes of the Han Chinese cohort (Taizhou longitudinal cohort [TZL], n = 2,964) and that in the Caucasian cohort (SALIA, n = 462) were obtained by on-site visits, whereas those collected in the National Survey of Physical Traits (NSPT) (n = 2,954) were obtained by scoring from standardized photographs of faces, hands, and arms. Double-blind evaluations were carried out for each individual, and the average scores were used in the subsequent analysis.

Genotyping

The Illumina Human OmniZhonghua8 V1.1 895k consists of 894,517 SNPs. Samples with call rate <98%, ambiguous sex, and duplicates were excluded. A total of 2,964 samples were kept in the TZL dataset. To detect population outliers, we assessed all the 2,964 participants together with two Uygur samples using EIGENSTRAT and found all the 2,964 Han Chinese samples gathered in a cluster. The top 10 principal components (PCs) of genetic variance were adjusted in GWAS to control population stratification. SNPs were excluded if they had a call rate < 98%, minor allele frequency (MAF) < 1%, and *P*-value of violations from Hardy–Weinberg equilibrium (P_{HWE}) < 0.001. After quality control, there were 802,328 SNPs and 2,964 samples left. Imputation was carried out using SHAPEIT2 and IMPUTE2, taking 1000 genome phase 3 as a reference. Imputed variants were then filtered with MAF > 0.01 and with an imputation quality score > 0.8 to produce the final dataset with 6,328,611 SNPs.

Genotyping of 2,954 Han Chinese in NSPT was performed using the Illumina Infinium Global Screening Array that analyzes over 710,000 SNPs. It is a fully custom array designed by WeGene (WeGene, Shanghai, China, https://www.wegene.com/). After the same criteria of quality control, 433,485 SNPs of 2,954 samples were left for further analysis. Imputation was done by SHAPEIT2 and IMPUTE2 using 1000 genome phase 3 as a reference. Imputed variants were filtered with MAF > 0.01, imputation quality score > 0.8, and violations from Hardy–Weinberg equilibrium ($P < 1 \times 10^{-5}$), leaving 8,042,915 variants. The top 10 PCs of genetic variance were adjusted in GWAS to control population stratification.

For genotyping in German, Affymetrix Axiom Precision Medicine Research Array was used and imputation was done by Minimac3 with 1000 Genome phase 3 reference panel. Individuals were filtered with a call rate >95% and identity by descent < 0.1. SNPs were filtered with call rate >95%, MAF >1%, $P_{(HWE)} > 10^{-6}$ and $R^2 > 0.3$. In summary, 462 samples and 9,665,096 SNPs remained in the analysis. The top 10 PCs of genetic variance were adjusted in GWAS to control population stratification.

DNA methylation

Bisulfite conversion of 500 ng of genomic DNA from each whole-blood sample was performed using the EZ DNA Methylation Kit (Zymo Research, Irvine, CA). Genome-wide DNA methylation was profiled on Infinium Human Methylation 850K EPIC BeadChip (Illumina, San Diego, CA) following the manufacturer's instructions. Samples were randomized with respect to slide and position on arrays, and all samples were hybridized and scanned concurrently to mitigate batch effects as recommended by the Illumina Infinium HD Assay Methylation Protocol Guide. Illumina.idat files were then processed with the minfi Bioconductor package (Aryee et al., 2014) without background correction. Probes with SNPs were removed using the dropLociWithSnps function from minfi. This function used the SNP information provided by Illumina and UCSC Common SNP tables (including version 132, 135, 137, 138, 141, 142, 144, 146, and 147) with preset MAF (0 is the default value and was used in this study) to filter SNP 5′-C-phosphate-G-3′ (CpG). We further removed probes on chromosomes X and Y. Then, we used the Illumina definition of beta-values and derived *P*-values for the detection of the rest of the probes by comparing the total intensity U + M with that of the background distribution (given by negative control probes), as implemented in minfi. Beta-values with $P > 0.01$ were set to missing. Only probes with less than 5% missing were retained. The missing beta-values were then imputed with the impute.knn function (using k = 5) from the impute R package. Type-2 probe bias was corrected using Beta Mixture Quantile normalization (Teschendorff et al., 2013). On the basis of PC analyses, we found a significant slide/beadchip effect. Therefore we used ComBat (Johnson et al., 2007) on M-values (logit of beta-values) to correct for the slide effect and then transformed the M-values back to beta-values.

Collection of melanin and erythema index

Melanin index and erythema index were measured by means of a Derma Spectrometer (Cortex Technology, Aalborg, Denmark) measured in the forehead area and the dorsal side of one upper arm for each individual in a subset (n = 1,851) of TZL.

Intrinsic epigenetic age acceleration calculation

Intrinsic epigenetic age acceleration was calculated as previously defined (Lu et al., 2018).

Expression quantitative trait loci from GTEx

Tissue-Specific All SNP Gene Associations (dbGaP accession number phs000424.v7.p2 on 01/15/2016) was downloaded from GTEx (https://gtexportal.org/home/datasets). Two datasets were used in this study: not sunexposed skin (suprapubic) and sunexposed skin (lower leg).

Trait variance captured by SNP

The SNP was extracted from PLINK bfile by –SNP and converted to additive genotype format by –recodeA. The trait

variance captured by the SNP (R^2) was calculated by linear regression model between non-facial SL and additive genotype data of the SNP in R platform.

Phenotypic and genetic correlation

The phenotypic correlation between composite phenotypes of facial and non-facial SLs was calculated by Pearson's correlation. The genetic correlation was calculated by Genome-wide Complex Trait Analysis.

Fine mapping and functional annotation of variants

First, we applied PAINTOR (Probabilistic Annotation INTegratOR) to calculate the Bayesian posterior causal probability for each variant and to identify the set of those variants that collectively explained 99% of the total probability. The reference functional annotations included epigenomes of 127 human tissues and cell types from the NIH Roadmap Epigenomics Mapping Consortium. Three epigenomic marks (H3K27ac, H3K4me1, and H3K4me3) were also included in our analysis. The posterior probability of each SNP was calculated by dividing the SNP's Bayes factor by the sum of the Bayes factors of all SNPs in the region. A 99% credible set was then constructed by (i) ranking all variants according to their Bayes factor and (ii) including ranked variants until their cumulative posterior probability of representing the causal variant at a given locus exceeded 0.99. Because the result obtained by PAINTOR strongly relies on the *P*-value, we used a second strategy to search for additional candidate SNPs with putative functional relevance. Specifically, we hypothesized that the functionally relevant variants would be in high linkage disequilibrium with rs2853672 (the target SNP suggested by PAINTOR) and located in close proximity to this SNP. We therefore prioritized 12 variants located in the ±5 kb region of rs2853672. We used Integrative Weighted scoring to evaluate the possible functional consequences of these variants by integrating 11 weighted scoring methods (Supplementary Table S17).

Plasmid construction and luciferase assays

Telomerase reverse transcriptase (TERT) promoter region was isolated from human genomic DNA using PCR, and the PCR products were cut with KpnI and XhoI or XhoI and HindIII restriction enzymes (New England Biolabs, Ipswich, MA), gel purified, and subcloned into pGL3-Enhancer Vector or pGL3-Promoter Vector (Promega, Madison, WI). A375, KB, and SK-MEL-2 cells were seeded for 24 hours before transfection in a 96-well plate with about 20% confluence. The cells in each well were transfected with 200 ng of the luciferase reporter plasmids and 10 ng Renilla luciferase reporter plasmids using Lipofectamin3000 (Life Technologies, Carlsbad, CA). Forty-eight hours after transfections, the cells were washed with PBS, and the firefly and Renila luciferase activities were measured with VICTOR X5 Multilabel Reader (PerkinElmer, Waltham, MA) using the Dual-Luciferase Report Assay (an affiliate of Promega (Beijing) Biotech Co., Ltd, Beijing, China).

Dual-luciferase transcriptional reporter assay

To investigate the regulatory properties of the identified CpG loci, dual-luciferase transcriptional reporter assay was conducted as previously described (Zhu et al., 2017). Double-strand DNA containing eight repeats of cg23827991 region (ATCCGGAT) was cloned into the CpG-free promoter vector containing the luciferase reporter (pCpGL-basic) (Klug and Rehli, 2006) to generate pCpGL-8X-TERT. Methylation of pCpGL-8X-TERT was generated by treatment with M.SssI CpG methyltransferase (New England Biolabs, Ipswich, MA) according to the manufacturer's instructions. The control condition (unmethylated) was treated equally but in the absence of any methyltransferase. DNA was then recovered by ethanol precipitation. The completeness of methylation was checked using methylation-sensitive restriction enzymes HpaII. For reporter gene expression assay, cells were cotransfected with two constructs: pCpGL-8X-TERT (methylated and unmethylated) and pTK-RL (an affiliate of Promega (Beijing) Biotech Co., Ltd) using Lipofectamine 2000 (Life Technologies, Carlsbad, CA); the original pCpGL-basic plasmid was used as a negative control. Cells were harvested 48 hours after transfection for luciferase reporter assay using the dual-luciferase reporter assay system (an affiliate of Promega (Beijing) Biotech Co., Ltd), and signals were recorded by calculating firefly luciferase activity normalized to renilla activity. All assays were repeated twice.

CRISPR/Cas9-mediated gene editing

For each candidate variant, single-guide RNAs (sgRNAs) were designed and cloned into the lentiCRISPR v2 vector and packaged into lentivirus as previously described (Sanjana et al., 2014). sgRNAs used for rs2853672 include AAGGGTTTTGCAGGTGCACG, and sgRNAs used for rs2736098 include sgRNA1 (CGCGGGCCCCCCATCCACATCG). We then transfected the sgRNAs plasmid into A375 cells using the Effectene reagent (Qiagen, Hilden, Germany). Forty-eight hours after transfection, the cells were selected on puromycin for 48 hours to eliminate untransfected cells. Successfully transfected cells were then diluted for colonial growth.

Telomere length measurement

To inspect the association between telomere length and SLs, telomere lengths were measured on a subset (n = 800) of individuals from the TZL dataset. People in the subset have a similar distribution of SLs scores as the complete dataset.

Genomic DNA was isolated from peripheral blood according to EltbioTMMahBeads DNA Extraction Kit. Relative mean telomere length was determined with qRT-PCR that compares telomere repeat copy number (T) with single-copy gene copy number (S) (T/S ratio) in a given sample as previously reported (Cawthon, 2002). All PCRs were performed on the ABI 7900 (Applied Biosystems, Foster City, CA).

In brief, two master mixes of PCR reagents were prepared, one for the telomere reaction and one for the single-copy gene reaction (acidic ribosomal phosphoprotein PO gene on chromosome 12). The primer sequences and thermal cycling profiles were given in detail as follows:

The primer sequences (written 5′→3′) were GGTTTTT GAGGGTGAGGGTGAGGGTGAGGGTGAGGGT for tel 1, TCCCGACTATCCCTATCCCTATCCCTATCCCTATCCCTA for tel 2, CAGCAAGTGGGAAGGTGTAATCC for 36B4u, and CCCATTCTATCATCAACGGGTACAA for 36B4d.

The thermal cycling profile for the telomere PCR consisted of the following steps: for stage 1, 95 °C for 10 minutes; for stage 2, 40 cycles of 95 °C for 15 seconds, 54 °C for 2 minutes, and 72 °C for 10 minutes with signal acquisition. Melt

curve analysis was performed at the end of each run to verify the specificity of PCR amplification products. Standard curves were included in each run ranging from 0.25 to 64 ng and prepared by two-fold serial dilutions of a peripheral blood genomic DNA sample, and the linear correlation coefficient (r^2) value for both reactions was >0.98.

Two-sample–based Mendelian randomization

Two-sample–based Mendelian randomization test was performed on the basis of R packages TwosampleMR (Hemani et al., 2018) and CAUSE (Morrison et al., 2020). The exposure summary statistics of TERT expression were downloaded from GTEX (https://www.gtexportal.org/home/datasets). The exposure summary statistics of telomere length; intrinsic epigenetic age acceleration; seborrhoeic keratosis; and pigmentation-related trait, that is, basal cell carcinoma, were downloaded from published resources (Adolphe et al., 2021; Bojesen et al., 2013; Codd et al., 2013; Dorajoo et al., 2019; Ghoussaini et al., 2021; Li et al., 2020; Lu et al., 2018; McCartney et al., 2021; Mountjoy et al., 2021; Pooley et al., 2013). Instrument SNPs for TwoSampleMR were selected on the basis of $P < 10^{-5}$ for leukocyte telomere length and intrinsic epigenetic age acceleration exposure summary data (Supplementary Tables S18 and S19). LD clumping (r2 < 0.001) was applied. We applied multiple-instrument approaches to mitigate the effect of confounders, and we chose the Mendelian randomization egger method to describe our results. The results from the other 13 methods from TwoSampleMR and CAUSE were also presented. Pleiotropy analysis was performed using Mendelian randomization egger methods, where $P_{\text{pleiotropy}} < 0.05$ indicated that there was a pleiotropic effect between exposure and outcome. We also calculated the power of detecting causality from leukocyte telomere length and intrinsic epigenetic age acceleration to SL on the basis of publicly available data (https://shiny.cnsgenomics.com/mRnd/).

Association between SL and environmental factors

In TZL, a series of environmental factors, including mean sun exposure time, skin care habits, dietary, education, and social-economic factors, were collected. Association analysis among these environmental factors and facial and nonfacial SL was carried out in TZL. A linear regression model was applied for each association analysis where age and sex were adjusted on the R platform.

Association between rs2853672 and SL in high and low sun-exposure groups

In TZL and NSPT, the amount of sun exposure for each sample in their past lives was also collected. The samples were grouped into high or low sun exposure according to the amount of sun exposure, for example, samples with an amount of sun exposure larger than 2 hours per day were grouped into the group of high exposure; otherwise, they were grouped into the group of low exposure. The associations between rs2853672 and facial and non-facial SL were carried out in PLINK 1.9 in each group, and linear regression and additive models were applied and adjusted for age, sex, and top 10 PCs.

Association between rs2853672 and SL in light and dark skin color groups

In TZL and NSPT, we also collected the skin color of each individual according to photo-measured mean values of L, A, and B (Wang et al., 2022). ITA° was calculated according to the following formula, where the larger the ITA°, the lighter the skin color.

$$\text{ITA}^\circ = \{\arctan[(\text{L} - 50)/\text{B}]\} \times 180/\pi$$

We take individuals with ITA° > 28 as light skin color (Ly et al., 2020) and those otherwise as dark skin color. Then, we explored the associations between TERT SNPs and non-facial SL in light and dark skin color groups in each data. This was done in PLINK 1.9, where linear regression and additive models were applied and adjusted for age, sex, and top 10 PCs.

Sensitivity analysis of GWASs

Distribution of phenotypes. The distributions of the composite phenotypes in TZL and NSPT, which are shown in Supplementary Figure S4a, are not normal but quite dispersed. It was difficult to normalize such data. We generated binary traits (composite phenotypes ≥ 0 or not) (Supplementary Figure S4b) in each cohort and carried out GWASs on these binary traits, which indicated similar results to those of the original composite phenotypes (Supplementary Figure S4c–f). Because the original composite phenotypes could better represent the severity of SL, we present the GWAS and meta-results of the original composite phenotypes in this study. We also extracted one single composite phenotype derived from the seven SL phenotypes and carried out an association analysis between TERT SNP (rs2853672) and the one single composite SL phenotype. The associations only reached nominal significance in both TZL and NSPT, suggesting lowered power when applying the single composite SL phenotype (Supplementary Table S20).

Relatedness. Although our datasets (TZL and NSPT) did not include family data, there are indeed a small number of related samples in our datasets. Precisely, we have 292 pairs of samples with identity by descent > 0.1875 in TZL and 744 pairs of samples with identity by descent > 0.1875 in NSPT. To explore the impact of the related samples on the results and main conclusions, we further dealt with relatedness in the samples by deleting 253 samples in TZL and 513 samples in NSPT to ensure identity by descent < 0.1875 in all the sample pairs. Subsequently, we reran all the relevant analyses, for example, GWASs, meta-analyses, and candidate gene analyses. We found that all the relevant results and conclusions remained valid, whereas only the detailed numbers were changed. The relevant results from the two strategies are included in Supplementary Tables S21–S24.

Consistency assessment of SCINEXA scores by in-person and photo rating

For the samples in TZL, we had SCINEXA scores generated by both in-person and photo ratings. We found that the performance of these two manners was in moderate to almost perfect agreement on the seven SL phenotypes (Kappa = 0.47–0.98) (Supplementary Figure S5).

SUPPLEMENTARY REFERENCES

Adolphe C, Xue A, Fard AT, Genovesi LA, Yang J, Wainwright BJ. Genetic and functional interaction network analysis reveals global enrichment of regulatory T cell genes influencing basal cell carcinoma susceptibility. Genome Med 2021;13:19.

Aryee MJ, Jaffe AE, Corrada-Bravo H, Ladd-Acosta C, Feinberg AP, Hansen KD, et al. Minfi: a flexible and comprehensive Bioconductor package for the analysis of Infinium DNA methylation microarrays. Bioinformatics 2014;30:1363–9.

Bojesen SE, Pooley KA, Johnatty SE, Beesley J, Michailidou K, Tyrer JP, et al. Multiple independent variants at the tert locus are associated with telomere length and risks of breast and ovarian cancer. Nat Genet 2013;45:371–84. 84.e1–2.

Cawthon RM. Telomere measurement by quantitative PCR. Nucleic acids research 2002;30:e47.

Codd V, Nelson CP, Albrecht E, Mangino M, Deelen J, Buxton JL, et al. Identification of seven loci affecting mean telomere length and their association with disease. Nat Genet 2013;45:422–7. 427e1–2.

Dorajoo R, Chang X, Gurung RL, Li Z, Wang L, Wang R, et al. Loci for human leukocyte telomere length in the Singaporean Chinese population and trans-ethnic genetic studies. Nat Commun 2019;10:2491.

Fuks KB, Hüls A, Sugiri D, Altug H, Vierkötter A, Abramson MJ, et al. Tropospheric ozone and skin aging: results from two German cohort studies. Environ Int 2019;124:139–44.

Gao W, Tan J, Hüls A, Ding A, Liu Y, Matsui MS, et al. Genetic variants associated with skin aging in the Chinese Han population. J Dermatol Sci 2017;86:21–9.

Ghoussaini M, Mountjoy E, Carmona M, Peat G, Schmidt EM, Hercules A, et al. Open Targets Genetics: systematic identification of trait-associated genes using large-scale genetics and functional genomics. Nucleic Acids Res 2021;49:D1311–20.

Hemani G, Zheng J, Elsworth B, Wade KH, Haberland V, Baird D, et al. The MR-Base platform supports systematic causal inference across the human phenome. eLife 2018;7.

Johnson WE, Li C, Rabinovic A. Adjusting batch effects in microarray expression data using empirical Bayes methods. Biostat (Oxf Engl) 2007;8:118–27.

Klug M, Rehli M. Functional analysis of promoter CpG methylation using a CpG-free luciferase reporter vector. Epigenetics 2006;1:127–30.

Li C, Stoma S, Lotta LA, Warner S, Albrecht E, Allione A, et al. Genome-wide association analysis in humans links nucleotide metabolism to leukocyte telomere length. Am J Hum Genet 2020;106:389–404.

Li M, Vierkötter A, Schikowski T, Hüls A, Ding A, Matsui MS, et al. Epidemiological evidence that indoor air pollution from cooking with solid fuels accelerates skin aging in Chinese women. J Dermatol Sci 2015;79:148–54.

Liu Y, Gao W, Koellmann C, Le Clerc S, Hüls A, Li B, et al. Genome-wide scan identified genetic variants associated with skin aging in a Chinese female population. J Dermatol Sci 2019;96:42–9.

Lu AT, Xue L, Salfati EL, Chen BH, Ferrucci L, Levy D, et al. GWAS of epigenetic aging rates in blood reveals a critical role for tert. Nat Commun 2018;9:387.

Ly BCK, Dyer EB, Feig JL, Chien AL, Del Bino S. Research Techniques Made Simple: Cutaneous Colorimetry: A Reliable Technique for Objective Skin Color Measurement. The Journal of investigative dermatology 2020;140:3–12. e1.

McCartney DL, Min JL, Richmond RC, Lu AT, Sobczyk MK, Davies G, et al. Genome-wide association studies identify 137 genetic loci for DNA methylation biomarkers of aging. Genome Biol 2021;22:194.

Morrison J, Knoblauch N, Marcus JH, Stephens M, He X. Mendelian randomization accounting for correlated and uncorrelated pleiotropic effects using genome-wide summary statistics. Nat Genet 2020;52:740–7.

Mountjoy E, Schmidt EM, Carmona M, Schwartzentruber J, Peat G, Miranda A, et al. An open approach to systematically prioritize causal variants and genes at all published human GWAS trait-associated loci. Nat Genet 2021;53:1527–33.

Pooley KA, Bojesen SE, Weischer M, Nielsen SF, Thompson D, Amin Al Olama A, et al. A genome-wide association scan (GWAS) for mean telomere length within the COGS project: identified loci show little association with hormone-related cancer risk. Hum Mol Genet 2013;22:5056–64.

Sanjana NE, Shalem O, Zhang F. Improved vectors and genome-wide libraries for CRISPR screening. Nat Methods 2014;11:783–4.

Teschendorff AE, Marabita F, Lechner M, Bartlett T, Tegner J, Gomez-Cabrero D, et al. A beta-mixture quantile normalization method for correcting probe design bias in Illumina Infinium 450 k DNA methylation data. Bioinformatics 2013;29:189–96.

Vierkötter A, Hüls A, Yamamoto A, Stolz S, Krämer U, Matsui MS, et al. Extrinsic skin ageing in German, Chinese and Japanese women manifests differently in all three groups depending on ethnic background, age and anatomical site. J Dermatol Sci 2016;83:219–25.

Vierkötter A, Ranft U, Krämer U, Sugiri D, Reimann V, Krutmann J. The SCINEXA: a novel, validated score to simultaneously assess and differentiate between intrinsic and extrinsic skin ageing. J Dermatol Sci 2009;53:207–11.

Vierkötter A, Schikowski T, Ranft U, Sugiri D, Matsui M, Krämer U, et al. Airborne particle exposure and extrinsic skin aging. J Invest Dermatol 2010;130:2719–26.

Wang F, Luo Q, Chen Y, Liu Y, Xu K, Adhikari K, et al. A Genome-Wide Scan on Individual Typology Angle Found Variants at SLC24A2 Associated with Skin Color Variation in Chinese Populations. The Journal of investigative dermatology 2022;142:1223–7. e14.

Zhu Z, Meng W, Liu P, Zhu X, Liu Y, Zou H. DNA hypomethylation of a transcription factor binding site within the promoter of a gout risk gene NRBP1 upregulates its expression by inhibition of TFAP2A binding. Clin Epigenetics 2017;9:99.

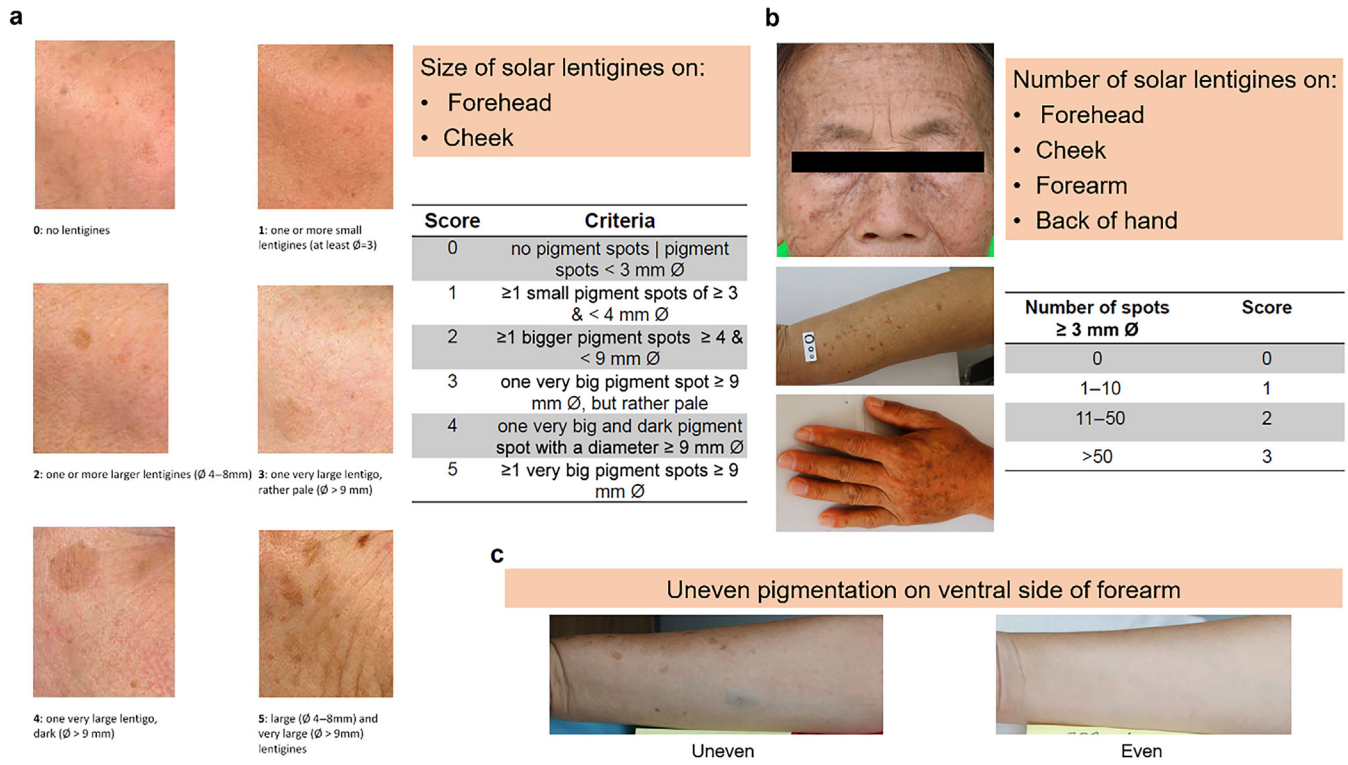

Supplementary Figure S1. Phenotyping methods of seven solar lentigines traits from SCINEXA. (**a**) Quantification of solar lentigines size on forehead and cheek. (**b**) Quantification of solar lentigines number on forehead, cheek, forearm, and back of the hand. (**c**) Quantification of uneven pigmentation on the ventral side of the forearm.

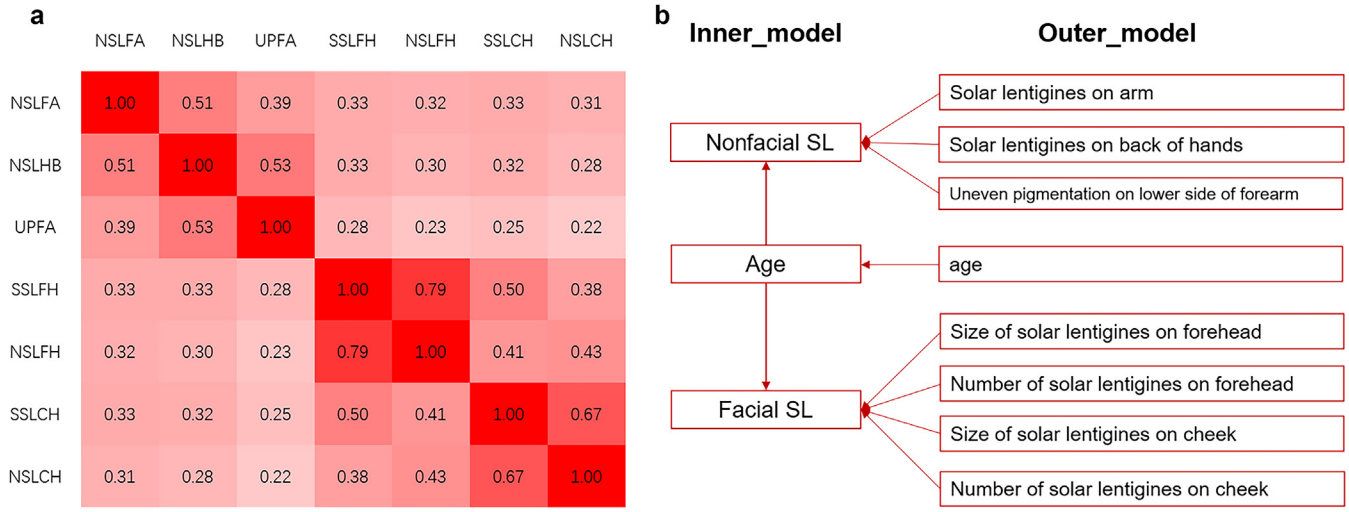

Supplementary Figure S2. Pearson correlation among seven SL traits and composite phenotype extraction of facial SLs. (**a**) Pearson correlation among seven SL phenotypes. (**b**) Composite phenotype extraction by partial least square path model. NSLCH, number of solar lentigines on the cheek; NSLFA, solar lentigines on the forearm; NSLFH, number of solar lentigines on the forehead; NSLHB, solar lentigines on the back of the hand; SL, solar lentigines; SSLCH, size of solar lentigines on the cheek; SSLFH, size of solar lentigines on the forehead; UPFA, uneven pigmentation on the lower side of the forearm.

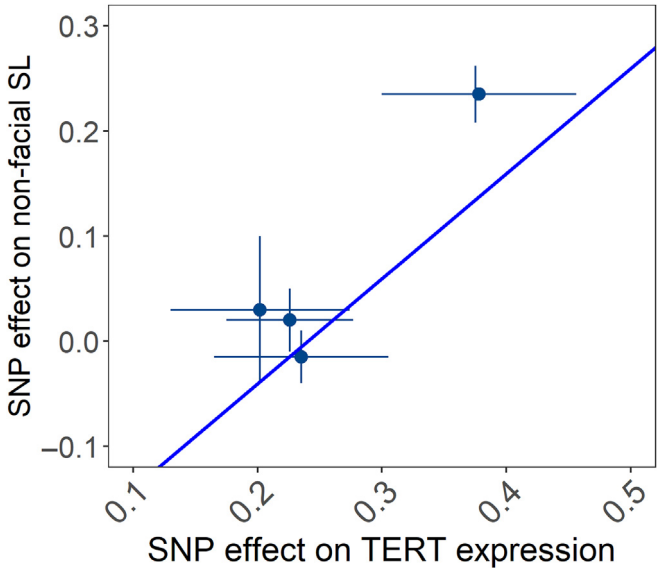

Supplementary Figure S3. Scatter plot of two-sample–based MR result between TERT expression and non-facial SL. MR, Mendelian randomization; SL, solar lentigines; TERT, telomerase reverse transcriptase.

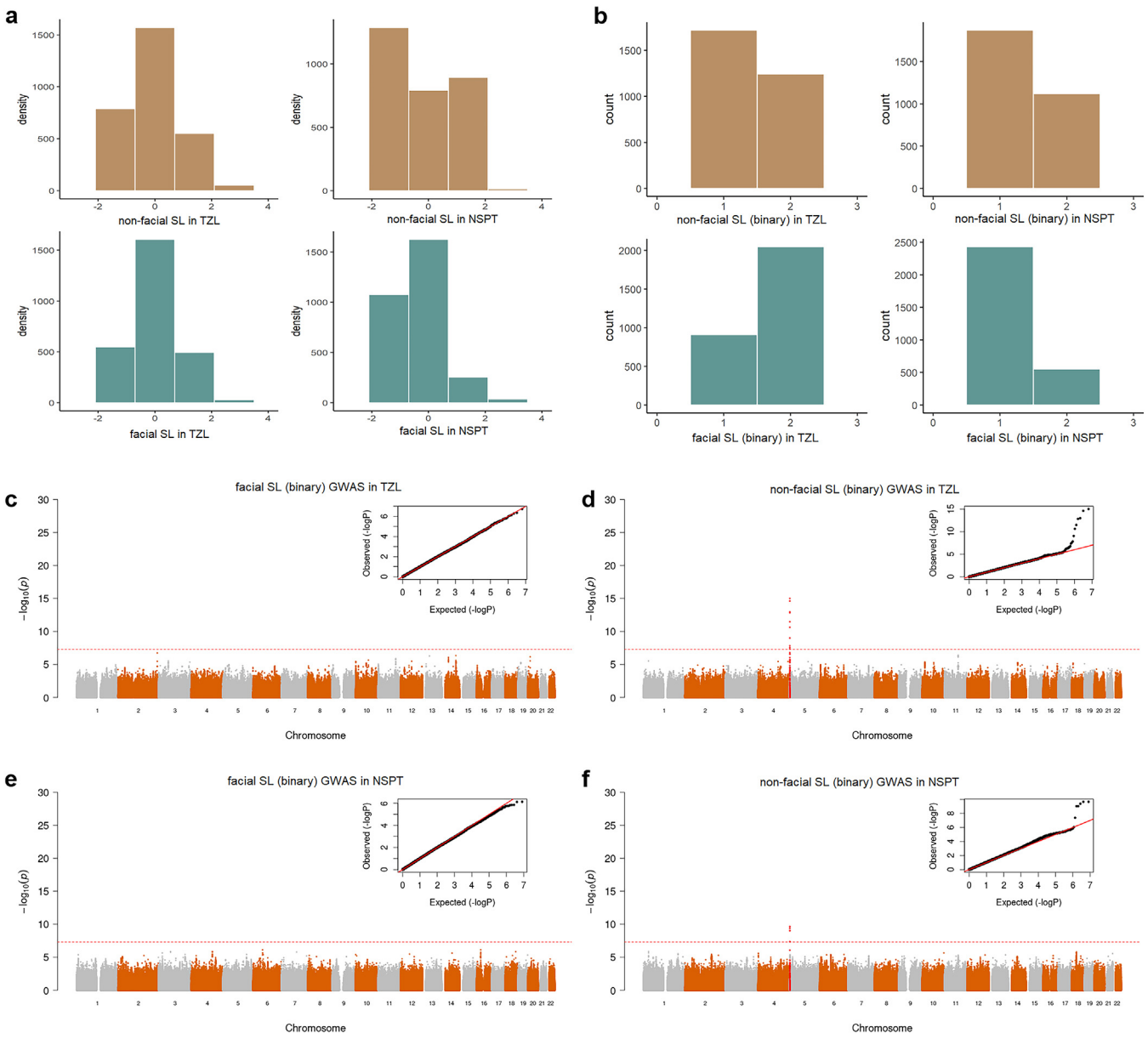

Supplementary Figure S4. The distribution and GWAS results of initial and binary composite phenotypes of facial and non-facial SL in TZL and NSPT. (**a**) The distribution of non-facial and facial SL composite phenotypes in TZL and NSPT. (**b**) The distribution of binary non-facial and facial SL composite phenotypes in TZL and NSPT. (**c–f**) The GWAS results of binary composite phenotypes of facial and non-facial SL in TZL and NSPT, respectively. NSPT, National Survey of Physical Traits; SL, solar lentigines; TZL, Taizhou longitudinal cohort.

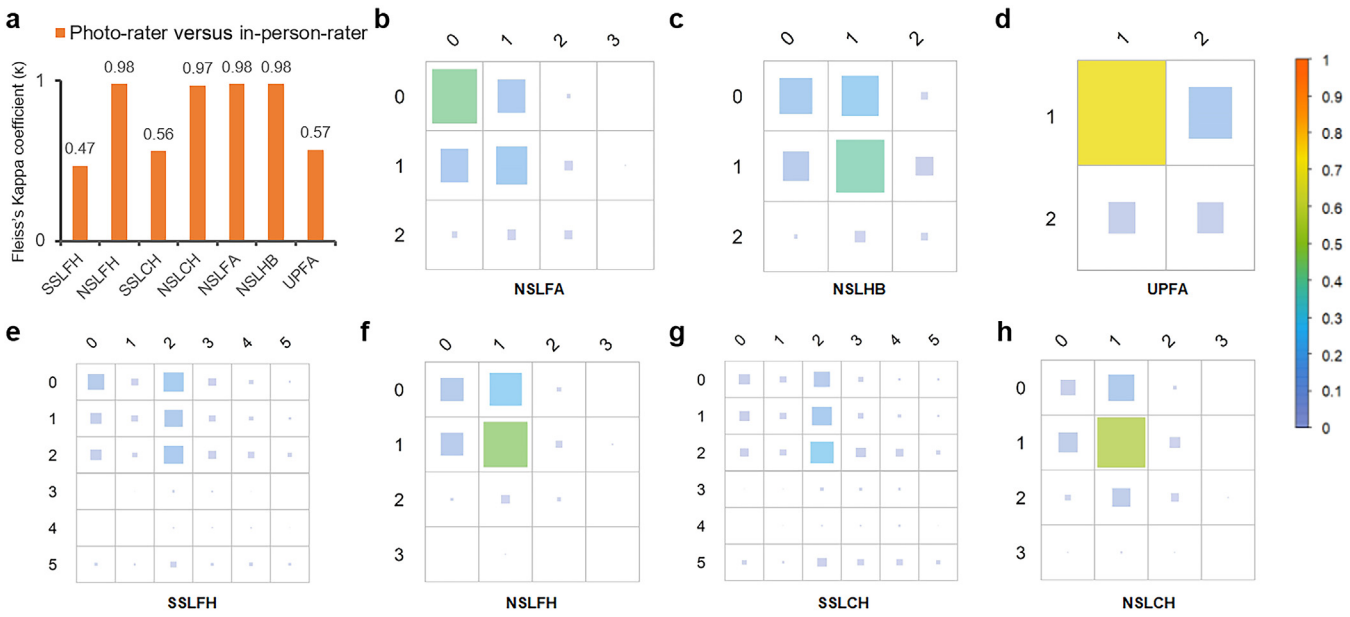

Supplementary Figure S5. The Fleiss's Kappa coefficient (κ) and concordance between in-person rating and photo rating in TZL. (**a**) The Fleiss's kappa coefficient (κ) of seven traits between in-person rating and photo rating: $\kappa < 0$, poor agreement; $\kappa = 0.01–0.20$, slight agreement; $\kappa = 0.21–0.40$, fair agreement; $\kappa = 0.41–0.60$, moderate agreement; $\kappa = 0.61–0.80$, substantial agreement; $\kappa = 0.81–1.00$, almost perfect agreement. (**b–h**) The heatmaps showed the concordance of each trait between in-person rating and photo rating. The size and color of each square represent the number and percentage of individuals included in the bin, respectively. The color bar is shown on the right side, that is, low percent (blue), medium percent (green), and high percent (red). NSLCH, number of solar lentigines on the cheek; NSLFA, solar lentigines on the forearm; NSLFH, number of solar lentigines on the forehead; NSLHB, solar lentigines on back of hands; SSLCH, size of solar lentigines on the cheek; SSLFH, size of solar lentigines on the forehead; TZL, Taizhou longitudinal cohort; UPFA, uneven pigmentation on the lower side of the forearm.

Supplementary Table S1. The Correlation and 95% CI among Seven SL Traits

		Pearson Correlation		Spearman Correlation		Kendell Correlation	
Trait 1	**Trait 2**	**rho**	**95% CI**	**rho**	**95% CI**	**Tau**	***P*-Value**
NSLFA	NSLHB	0.50	0.48–0.53	0.49	0.47–0.52	0.48	$<2.2 \times 10^{-16}$
NSLFA	UPFA	0.38	0.35–0.42	0.37	0.34–0.4	0.36	$<2.2 \times 10^{-16}$
NSLFA	SSLFH	0.33	0.30–0.37	0.33	0.29–0.36	0.30	$<2.2 \times 10^{-16}$
NSLFA	NSLFH	0.32	0.29–0.35	0.32	0.29–0.36	0.31	$<2.2 \times 10^{-16}$
NSLFA	SSLCH	0.34	0.30–0.37	0.33	0.3–0.36	0.30	$<2.2 \times 10^{-16}$
NSLFA	NSLCH	0.31	0.28–0.35	0.31	0.28–0.35	0.30	$<2.2 \times 10^{-16}$
NSLHB	UPFA	0.53	0.50–0.55	0.51	0.48–0.54	0.50	$<2.2 \times 10^{-16}$
NSLHB	SSLFH	0.33	0.30–0.36	0.31	0.28–0.34	0.29	$<2.2 \times 10^{-16}$
NSLHB	NSLFH	0.30	0.27–0.33	0.3	0.27–0.33	0.29	$<2.2 \times 10^{-16}$
NSLHB	SSLCH	0.33	0.29–0.36	0.31	0.28–0.34	0.29	$<2.2 \times 10^{-16}$
NSLHB	NSLCH	0.29	0.25–0.32	0.28	0.25–0.31	0.27	$<2.2 \times 10^{-16}$
UPFA	SSLFH	0.28	0.25–0.32	0.28	0.25–0.31	0.26	$<2.2 \times 10^{-16}$
UPFA	NSLFH	0.23	0.19–0.26	0.22	0.19–0.25	0.22	$<2.2 \times 10^{-16}$
UPFA	SSLCH	0.25	0.22–0.29	0.25	0.21–0.28	0.23	$<2.2 \times 10^{-16}$
UPFA	NSLCH	0.21	0.18–0.25	0.21	0.18–0.24	0.21	$<2.2 \times 10^{-16}$
SSLFH	NSLFH	0.80	0.78–0.81	0.81	0.79–0.83	0.75	$<2.2 \times 10^{-16}$
SSLFH	SSLCH	0.50	0.47–0.52	0.48	0.45–0.51	0.43	$<2.2 \times 10^{-16}$
SSLFH	NSLCH	0.38	0.35–0.41	0.39	0.36–0.42	0.36	$<2.2 \times 10^{-16}$
NSLFH	SSLCH	0.41	0.38–0.44	0.42	0.39–0.45	0.39	$<2.2 \times 10^{-16}$
NSLFH	NSLCH	0.43	0.40–0.46	0.42	0.39–0.46	0.42	$<2.2 \times 10^{-16}$
SSLCH	NSLCH	0.66	0.64–0.68	0.66	0.63–0.68	0.61	$<2.2 \times 10^{-16}$

Abbreviations: CI, confidence interval; NSLCH, number of solar lentigines on the cheek; NSLFA, solar lentigines on the forearm; NSLFH, number of solar lentigines on the forehead; NSLHB, solar lentigines on the back of hands; SL, solar lentigines; SSLCH, size of solar lentigines on the cheek; SSLFH, size of solar lentigines on the forehead; UPFA, uneven pigmentation on the lower side of the forearm.

Supplementary Table S2. The Heritability Estimated from GCTA-LDMS for Single Traits and Composite Phenotype of SL in TZL and NSPT

Phenotype	TZL (%)	NSPT (%)
Solar lentigines on the arm	21 ± 13	39 ± 8
Solar lentigines on the back of hands	36 ± 13	38 ± 8
Uneven pigmentation on the lower side of the forearm	24 ± 14	44 ± 8
Composite phenotype of nonfacial SL	**32 ± 13**	**42 ± 8**
Size of solar lentigines on the forehead	33 ± 12	26 ± 9
Number of solar lentigines on the forehead	23 ± 12	34 ± 9
Size of solar lentigines on the cheek	16 ± 12	36 ± 8
Number of solar lentigines on the cheek	33 ± 12	40 ± 8
Composite phenotype of facial SL	**36 ± 11**	**43 ± 8**

Abbreviations: GCTA, Genome-wide Complex Trait Analysis; LDMS, linkage disequilibrium and minor allele frequency stratified; NSPT, National Survey of Physical Traits; SL, solar lentigines; TZL, Taizhou longitudinal cohort.
Boldfaces indicate composite phenotypes.

Supplementary Table S3. Significant SNPs Associated with Non-facial SL Adjusted for Relatedness by GCTA (fastGWA)

				Meta			Discovery 1 (TZL)			Discovery 2 (NSPT)			Replication (SALIA)		
CHR	BP	SNP	A1	Beta	SE	*P*-Value	Beta	SE	*P*-Value	Beta	SE	*P*-Value	Beta	SE	*P*-Value
5	1276050	rs113136187	t	0.12	0.02	3.25×10^{-11}	0.14	0.03	1.46×10^{-7}	0.10	0.02	4.68×10^{-5}	0.19	0.13	0.15
5	1279790	rs10069690	t	−0.13	0.02	1.40×10^{-12}	−0.15	0.03	6.04×10^{-8}	−0.12	0.03	4.00×10^{-6}	−0.11	0.11	0.32
5	1279964	rs10054203	c	−0.09	0.01	3.92×10^{-10}	−0.12	0.02	4.00×10^{-8}	−0.06	0.02	5.56×10^{-4}	−0.11	0.10	0.27
5	1280028	rs2242652	a	−0.14	0.02	9.41×10^{-14}	−0.16	0.03	4.18×10^{-9}	−0.12	0.03	4.91×10^{-6}	−0.20	0.13	0.11
5	1280128	rs7734992	t	0.10	0.01	1.20×10^{-12}	0.12	0.02	1.57×10^{-8}	0.08	0.02	2.31×10^{-5}	0.21	0.10	0.03
5	1280830	rs4975538	c	−0.10	0.01	4.34×10^{-12}	−0.12	0.02	1.46×10^{-8}	−0.08	0.02	3.51×10^{-5}	−0.13	0.10	0.18
5	1280938	rs6897196	a	0.10	0.01	2.06×10^{-12}	−0.12	0.02	1.33×10^{-8}	−0.08	0.02	1.98×10^{-5}	−0.13	0.10	0.18
5	1282319	rs7726159	a	−0.10	0.01	2.71×10^{-13}	−0.12	0.02	4.75×10^{-9}	−0.09	0.02	5.07×10^{-6}	−0.09	0.10	0.36
5	1282414	rs7725218	a	−0.10	0.01	7.52×10^{-13}	−0.12	0.02	7.14×10^{-9}	−0.08	0.02	9.92×10^{-6}	−0.10	0.10	0.31
5	1283312	rs7713218	a	−0.11	0.01	2.22×10^{-16}	−0.14	0.02	1.44×10^{-10}	−0.10	0.02	5.40×10^{-8}	−0.02	0.10	0.83
5	1283486	rs7717443	t	−0.11	0.01	3.94×10^{-16}	−0.13	0.02	2.33×10^{-10}	−0.10	0.02	6.46×10^{-8}	−0.02	0.10	0.83
5	1283755	rs72709458	t	−0.15	0.02	5.53×10^{-16}	−0.19	0.03	4.53×10^{-12}	−0.11	0.02	6.23×10^{-6}	−0.20	0.12	0.09
5	1284135	rs4449583	t	−0.10	0.01	2.68×10^{-13}	−0.13	0.02	1.48×10^{-9}	−0.08	0.02	1.12×10^{-5}	−0.10	0.10	0.34
5	1285162	rs10866498	t	0.12	0.01	1.22×10^{-16}	0.14	0.02	1.67×10^{-11}	0.10	0.02	2.04×10^{-7}	0.05	0.10	0.58
5	1285974	rs7705526	a	−0.11	0.01	1.48×10^{-14}	−0.13	0.02	1.02×10^{-9}	−0.09	0.02	4.85×10^{-6}	−0.25	0.10	0.01
5	1286516	rs2736100	a	0.14	0.01	7.48×10^{-23}	0.16	0.02	8.79×10^{-15}	0.11	0.02	5.44×10^{-9}	0.33	0.10	5.76×10^{-4}
5	1287194	rs2853677	a	0.16	0.01	3.04×10^{-28}	0.19	0.02	1.36×10^{-18}	0.13	0.02	3.45×10^{-11}	0.28	0.10	3.91×10^{-3}
5	1287340	rs2736099	a	−0.18	0.01	5.30×10^{-37}	−0.21	0.02	3.18×10^{-23}	−0.15	0.02	5.12×10^{-15}	−0.31	0.09	1.02×10^{-3}
5	1287505	rs7710703	t	−0.22	0.02	4.72×10^{-22}	−0.26	0.04	6.63×10^{-13}	−0.18	0.03	1.42×10^{-9}	−0.53	0.14	2.17×10^{-4}
5	1288547	rs2853676	t	−0.19	0.02	1.76×10^{-25}	−0.23	0.03	2.70×10^{-16}	−0.15	0.02	7.07×10^{-10}	−0.39	0.11	2.57×10^{-4}
5	1289880	rs62332588	t	−0.17	0.01	3.31×10^{-34}	−0.21	0.02	2.30×10^{-22}	−0.14	0.02	6.52×10^{-14}	−0.24	0.09	0.01
5	1289975	rs74682426	a	−0.21	0.02	2.51×10^{-20}	−0.26	0.04	9.80×10^{-14}	−0.16	0.03	5.24×10^{-8}	−0.42	0.14	2.54×10^{-3}
5	1290319	rs62332591	t	−0.18	0.01	6.50×10^{-38}	−0.21	0.02	1.99×10^{-24}	−0.15	0.02	6.45×10^{-15}	−0.31	0.09	8.44×10^{-4}
5	1291735	rs56158232	a	0.16	0.02	2.50×10^{-21}	0.19	0.03	1.07×10^{-12}	0.14	0.02	4.11×10^{-10}	0.23	0.12	0.05
5	1291740	rs56023411	t	0.15	0.02	1.23×10^{-19}	0.19	0.03	1.07×10^{-12}	0.13	0.02	1.12×10^{-8}	0.23	0.12	0.05
5	**1292983**	**rs2853672**	**a**	**0.19**	**0.01**	$\mathbf{4.93 \times 10^{-44}}$	**0.23**	**0.02**	$\mathbf{1.32 \times 10^{-28}}$	**0.15**	**0.02**	$\mathbf{3.66 \times 10^{-17}}$	**0.32**	**0.09**	$\mathbf{7.41 \times 10^{-4}}$
5	1294086	rs2736098	t	−0.12	0.01	1.09×10^{-17}	−0.15	0.02	1.47×10^{-12}	−0.10	0.02	4.55×10^{-7}	−0.20	0.11	0.06
5	1295349	rs2853669	a	0.12	0.01	1.37×10^{-16}	0.15	0.02	2.20×10^{-12}	0.09	0.02	1.48×10^{-6}	0.13	0.10	0.22
5	1296072	rs7712562	a	−0.20	0.02	1.16×10^{-18}	−0.23	0.04	8.37×10^{-11}	−0.17	0.03	1.56×10^{-8}	−0.43	0.14	2.39×10^{-3}
5	1296486	rs2735940	a	−0.18	0.01	4.73×10^{-41}	−0.21	0.02	2.93×10^{-25}	−0.15	0.02	5.35×10^{-17}	−0.32	0.09	6.78×10^{-4}
5	1296759	rs2736109	t	−0.09	0.01	1.25×10^{-9}	−0.11	0.02	6.61×10^{-7}	−0.08	0.02	1.42×10^{-4}	−0.03	0.10	0.77
5	1297258	rs6554754	t	−0.19	0.02	3.92×10^{-18}	−0.22	0.04	2.68×10^{-10}	−0.17	0.03	9.90×10^{-9}	−0.41	0.15	0.01
5	1297488	rs2736108	t	−0.10	0.02	6.25×10^{-11}	−0.11	0.02	8.44×10^{-7}	−0.09	0.02	2.24×10^{-5}	−0.15	0.10	0.16
5	1297854	rs2736107	t	−0.09	0.02	4.69×10^{-9}	−0.10	0.02	1.15×10^{-5}	−0.08	0.02	1.30×10^{-4}	−0.13	0.10	0.23
5	1297918	rs7449190	t	−0.18	0.02	1.02×10^{-18}	−0.20	0.03	1.64×10^{-10}	−0.16	0.03	7.46×10^{-9}	−0.43	0.14	2.39×10^{-3}
5	1299859	rs13174814	c	0.10	0.01	1.28×10^{-12}	0.10	0.02	5.65×10^{-6}	0.10	0.02	2.08×10^{-7}	0.25	0.11	0.02
5	1299862	rs13174919	c	0.09	0.01	1.35×10^{-11}	0.09	0.02	1.84×10^{-5}	0.09	0.02	5.08×10^{-7}	0.21	0.11	0.05
5	1300310	rs4975612	t	0.10	0.01	3.23×10^{-12}	0.09	0.02	3.80×10^{-5}	0.10	0.02	7.18×10^{-8}	0.26	0.11	0.02
5	1300429	rs2735946	t	−0.13	0.02	7.93×10^{-9}	−0.12	0.04	7.81×10^{-4}	−0.13	0.03	1.23×10^{-5}	−0.20	0.10	0.06
5	1343794	rs10462706	t	0.08	0.01	9.25×10^{-9}	0.09	0.02	6.34×10^{-5}	0.07	0.02	6.54×10^{-5}	0.20	0.13	0.11
15	28197037	rs1800414	t	−0.08	0.01	4.57×10^{-8}	−0.10	0.02	5.46×10^{-6}	−0.06	0.02	7.98×10^{-4}	−0.32	1.00	0.75

Abbreviations: BP, base position; CHR, chromosome; GCTA, Genome-wide Complex Trait Analysis; NSPT, National Survey of Physical Traits; SE, standard error; SL, solar lentigines; TZL, Taizhou longitudinal cohort.

Boldfaces indicated the top SNP associated with nonfacial SL in our study

Supplementary Table S4. Replication of GWAS Signals of Non-facial SL when Adjusted for Skin Color

				Adjust Skin Color (n = 1,852 Han Chineses)		
CHR	**BP**	**SNP**	**A1**	**Beta**	**SE**	***P*-Value**
5	1276050	rs113136187	t	0.15	0.03	1.86×10^{-5}
5	1279790	rs10069690	t	−0.15	0.03	9.72×10^{-6}
5	1279964	rs10054203	c	−0.12	0.03	8.52×10^{-6}
5	1280028	rs2242652	a	−0.16	0.03	3.05×10^{-6}
5	1280128	rs7734992	t	0.12	0.03	1.13×10^{-5}
5	1280830	rs4975538	c	−0.12	0.03	9.81×10^{-6}
5	1280938	rs6897196	a	0.12	0.03	8.76×10^{-6}
5	1282319	rs7726159	a	−0.14	0.03	4.71×10^{-7}
5	1283312	rs7713218	a	−0.15	0.03	1.66×10^{-8}
5	1283486	rs7717443	t	−0.15	0.03	1.93×10^{-8}
5	1283755	rs72709458	t	−0.20	0.03	1.95×10^{-8}
5	1284135	rs4449583	t	−0.14	0.03	1.76×10^{-7}
5	1285162	rs10866498	t	0.16	0.03	8.99×10^{-9}
5	1285974	rs7705526	a	−0.14	0.03	4.01×10^{-7}
5	1286516	rs2736100	a	0.19	0.03	8.75×10^{-12}
5	1287194	rs2853677	a	0.21	0.03	2.46×10^{-14}
5	1287505	rs7710703	t	−0.25	0.05	1.10×10^{-7}
5	1289880	rs62332588	t	−0.23	0.03	5.08×10^{-17}
5	1289975	rs74682426	a	−0.24	0.05	1.64×10^{-7}
5	1290319	rs62332591	t	−0.23	0.03	5.10×10^{-18}
5	1291735	rs56158232	a	0.18	0.03	2.25×10^{-7}
5	1291740	rs56023411	t	0.18	0.03	2.25×10^{-7}
5	**1292983**	**rs2853672**	**a**	**0.25**	**0.03**	$\mathbf{4.57 \times 10^{-21}}$
5	1294086	rs2736098	t	−0.19	0.03	4.93×10^{-11}
5	1295349	rs2853669	a	0.19	0.03	3.15×10^{-11}
5	1296072	rs7712562	a	−0.21	0.05	4.05×10^{-6}
5	1296486	rs2735940	a	−0.24	0.03	1.78×10^{-18}
5	1296759	rs2736109	t	−0.15	0.03	1.92×10^{-7}
5	1297258	rs6554754	t	−0.21	0.05	4.91×10^{-6}
5	1297488	rs2736108	t	−0.14	0.03	1.17×10^{-6}
5	1297854	rs2736107	t	−0.13	0.03	9.26×10^{-6}
5	1297918	rs7449190	t	−0.19	0.04	3.79×10^{-6}
5	1299859	rs13174814	c	0.12	0.03	2.27×10^{-5}
5	1300310	rs4975612	t	0.12	0.03	8.59×10^{-6}
5	1343794	rs10462706	t	0.13	0.03	6.53×10^{-6}
15	28196145	rs76930569	t	0.09	0.03	1.73×10^{-3}
15	28197037	rs1800414	t	−0.09	0.03	1.54×10^{-3}

Abbreviations: BP, base position; SL, solar lentigines.
Boldface indicated the top SNP associated with nonfacial SL in our study.

Supplementary Table S5. The Association between *TERT* SNP rs2853672 and Non-facial SLs in Dark and Light Skin Color Groups in TZL and NSPT

Cohort	**Skin Pigmentation**	**n**	**Beta**	**SE**	**t-Value**	***P*-Value**
TZL	Dark skin color	1,565	−0.22	0.03	−7.38	2.58×10^{-13}
TZL	Light skin color	1,066	−0.24	0.03	−7.39	2.89×10^{-13}
NSPT	Dark skin color	1,774	−0.15	0.02	−6.27	4.43×10^{-10}
NSPT	Light skin color	913	−0.15	0.03	−5.07	4.93×10^{-7}

Abbreviations: SE, standard error; NSPT, National Survey of Physical Traits; SL, solar lentigines; TERT, telomerase reverse transcriptase; TZL, Taizhou longitudinal cohort.

Supplementary Table S6. Replication of Candidate SNPs Detected in Previous Four SL-based GWASs Adjusted for Relatedness by GCTA (fastGWA)

						Replication in Han Chinese (TZL + NSPT)				
							Facial SL		Nonfacial SL	
Study	**CHR**	**Gene**	**SNP**	**EAF (EA)[1]**	**Beta/Log (OR)**	**EAF**	**Beta**	***P*-Value**	**Beta**	***P*-Value**
Dutch GWAS (Jacobs et al., 2015) (n = 2,844)	6	*IRF4*	rs12203592	0.09 (T)	0.44	<0.01	—	—	—	—
	9	*BNC2*	rs62543565	0.37 (C)	−0.15	0.68	0.01	0.30	−0.01	0.44
	16	*MC1R*	rs35063026	0.07 (T)	0.33	<0.01	—	—	—	—
	20	*RALY/ASIP*	rs6059655	0.08 (A)	0.3	<0.01	—	—	—	—
French GWAS (Laville et al., 2016) (n = 502)	6	*6p21* intergenic	rs9350204	0.15 (C)	—	0.37	0.005	0.73	0.02	0.14
			rs9358294	0.15 (G)	—	0.36	0.004	0.77	0.02	0.15
	6	*HLC-C* (near gene)	rs2853949	0.14 (A)	—	0.01	−0.03	0.66	−0.07	0.42
	6	*USP8P1*	rs2844614	0.14 (A)	—	0.01	−0.03	0.66	−0.07	0.42
			rs2844613	0.14 (T)	—	0.01	−0.03	0.66	−0.07	0.42
			rs2524069	0.13 (T)	—	0.02	−0.04	0.50	−0.11	0.10
			rs2853947	0.14 (T)	—	0.03	−0.07	0.12	−0.05	0.27
			rs2524067	0.14 (G)	—	0.03	−0.07	0.12	−0.05	0.27
			rs2524065	0.14 (C)	—	0.03	−0.07	0.12	−0.05	0.27
Japanese GWAS (Endo et al., 2018) (n = 11,311)	**5**	***PPARGC1B***	**rs251468**	**0.18 (T)**	**−0.11**	**0.21**	**−0.07**	**4.63×10^{-5}**	**−0.06**	**8.49×10^{-4}**
	9	*BNC2*	rs10810635	0.47 (T)	−0.12	0.72	−0.03	0.02	−0.03	0.11
	10	***RAB11FIP2***	**rs61866017**	**0.16 (T)**	**−0.11**	**0.12**	−0.04	0.05	**−0.07**	**1.10×10^{-3}**
			rs35563099	**0.09 (T)**	**−0.11**	**0.1**	−0.05	0.03	**−0.10**	**4.38×10^{-5}**
			rs10444039	**0.09 (A)**	**−0.22**	**0.1**	−0.05	0.02	**−0.09**	**4.54×10^{-5}**
			rs10886142	0.49 (T)	0.08	0.45	0.01	0.55	0.01	0.44
			rs4752116	0.21 (T)	−0.09	0.21	−0.02	0.13	−0.04	0.01
	10	***HSPA12A***	**rs12259842**	**0.25 (T)**	**0.09**	**0.21**	0.04	0.02	**0.08**	**4.02×10^{-6}**
	17	*AKAP1/MSI2*	rs17833789	0.45 (C)	0.07	0.48	0.02	0.26	0.003	0.83
Korean GWAS (Shin et al., 2021) (n = 17,019)	2	*LINC01877*	rs12693889	0.50 (T)	0.6	0.45	0.02	0.13	0.03	0.02
	5	*PPARGC1B*	rs32579	0.30 (T)	−1.56	0.35	−0.04	0.01	−0.03	0.08
	9	*BNC2*	rs16935073	0.43 (C)	1.58	0.3	0.04	0.01	0.03	0.07
	9	*CDKN2B-AS1*	rs643319	0.36 (A)	−0.54	0.36	0.02	0.12	0.01	0.60
	10	***10q26***	**rs11198112**	**0.10 (T)**	**−2.3**	**0.1**	−0.05	0.01	**−0.09**	**7.62×10^{-5}**
	16	*MC1R*	rs2228479	0.14 (A)	1.55	0.21	0.02	0.51	0.05	0.06
	19	***MFSD12***	**rs2240751**	**0.34 (G)**	**−0.67**	**0.29**	**−0.07**	**4.83×10^{-6}**	0.0003	0.98

Abbreviations: CHR, chromosome; EAF, effect allele frequency; GCTA, Genome-wide Complex Trait Analysis; NSPT, National Survey of Physical Traits; SL, solar lentigines; TZL, Taizhou longitudinal cohort.

Boldfaces indicate SNP replicated in our study at a *P*-value threshold of $0.05/29 = 1.72 \times 10^{-3}$.

[1]Denotes EAF in the original GWAS, and EA denotes the effect allele in the original GWAS.

Supplementary Table S7. Association between the Top Three Haplotypes and Composite Phenotype in the Chinese Combined Dataset and German Replication Dataset

Haplotype	**Study**	***P*-Value**	**Effect**	**Frequency**
H1:ACAGG	Chinese combined[1]	1.2×10^{-35}	0.185	0.507
	German replication[2]	4.4×10^{-4}	0.333	0.476
H2:CCAAA	Chinese combined	1.2×10^{-14}	−0.184	0.108
	German replication	2.4×10^{-3}	−0.428	0.122
H3:CTGGA	Chinese combined	2.1×10^{-15}	−0.123	0.359
	German replication	0.07	−0.192	0.290

Abbreviations: NSPT, National Survey of Physical Traits; TZL, Taizhou longitudinal cohort.

[1]Combination of TZL and NSPT dataset

[2]German sample of 462 individuals from SALIA cohort

Supplementary Table S8. Expression Quantitative Trait Loci for *TERT* Gene Expression in Skin Tissues Reported in Public Database (GTEx)

SNP	*P*-Value	Effect	Tissue
rs10073340	1.10×10^{-4}	−0.26	Skin - sunexposed (lower leg)
rs12332579	2.60×10^{-5}	0.29	Skin - sunexposed (lower leg)
rs1801075	9.70×10^{-5}	0.26	Skin - Sunexposed (lower leg)
rs2735940	**5.50×10^{-6}**	**0.23**	**Skin - Sunexposed (lower leg)**
rs2736100	**4.80×10^{-5}**	**0.23**	**Skin - not sunexposed (suprapubic)**
rs2853672	**9.50×10^{-6}**	**0.22**	**Skin - sunexposed (lower leg)**
rs2853676	**2.00×10^{-6}**	**0.28**	**Skin - sunexposed (lower leg)**
rs2853676	**3.90×10^{-6}**	**0.29**	**Skin - not sunexposed (suprapubic)**
rs2853677	**1.60×10^{-5}**	**0.24**	**Skin - not sunexposed (suprapubic)**
rs2853677	**2.60×10^{-5}**	**0.21**	**Skin - sunexposed (lower leg)**
rs34880677	2.90×10^{-5}	−0.29	Skin - sunexposed (lower leg)
rs35595862	8.00×10^{-5}	−0.27	Skin - sunexposed (lower leg)
rs6554754	**2.40×10^{-5}**	**0.35**	**Skin - not sunexposed (suprapubic)**
rs6554754	**2.50×10^{-5}**	**0.32**	**Skin - sunexposed (lower leg)**
rs7449190	**9.80×10^{-6}**	**0.35**	**Skin - not sunexposed (suprapubic)**
rs7449190	**1.90×10^{-5}**	**0.31**	**Skin - Sunexposed (lower leg)**
rs7710703	**1.70×10^{-5}**	**0.35**	**Skin - not sunexposed (suprapubic)**
rs7712562	**3.70×10^{-6}**	**0.36**	**Skin - not sunexposed (suprapubic)**
rs7712562	**7.20×10^{-6}**	**0.32**	**Skin - sunexposed (lower leg)**

Abbreviations: SL, solar lentigines; TERT, telomerase reverse transcriptase.
Boldfaces indicated SNP discovered in our GWAS of composite phenotype of SL on hand/arm.

Supplementary Table S9. Power of Associations between *TERT* SNPs and LTL and IEAA

	LTL					IEAA				
SNP	n	MAF	Beta	*P*-Value	Power	n	MAF	Beta	*P*-Value	Power
rs113136187	800	0.21	−0.64	0.19	0.24	3,523	0.18	0.27	0.07	0.15
rs10069690	800	0.21	−0.79	0.10	0.36	3,523	0.16	0.30	0.04	0.51
rs10054203	800	0.43	−0.24	0.54	0.09	3,523	0.40	0.56	5.36×10^{-7}	1.00
rs2242652	800	0.21	−0.85	0.08	0.40	3,523	0.16	0.35	0.02	0.63
rs7734992	800	0.42	−0.34	0.38	0.13	3,523	0.39	0.62	4.24×10^{-8}	1.00
rs4975538	800	0.41	−0.29	0.46	0.11	3,523	0.38	0.56	6.40×10^{-7}	1.00
rs6897196	800	0.41	−0.37	0.34	0.15	3,523	0.38	0.57	3.96×10^{-7}	1.00
rs7726159	800	0.43	0.05	0.90	0.05	3,523	0.38	0.65	1.17×10^{-8}	1.00
rs7713218	800	0.45	−0.03	0.95	0.05	3,523	0.41	0.54	1.37×10^{-6}	1.00
rs7717443	800	0.45	−0.02	0.96	0.05	3,523	0.40	0.53	2.00×10^{-6}	1.00
rs72709458	800	0.21	−0.74	0.13	0.32	3,523	0.17	0.41	5.66×10^{-3}	0.78
rs4449583	800	0.43	0.02	0.96	0.05	3,523	0.38	0.67	3.58×10^{-9}	1.00
rs10866498	800	0.46	−0.12	0.76	0.06	3,523	0.42	0.49	1.14×10^{-5}	0.99
rs7705526	800	0.43	−0.10	0.80	0.06	3,523	0.39	0.67	3.21×10^{-9}	1.00
rs2736100	800	0.44	−0.19	0.63	0.07	3,523	0.41	0.54	1.55×10^{-6}	1.00
rs2853677	800	0.40	−0.06	0.88	0.05	3,523	0.38	0.49	1.52×10^{-5}	0.99
rs7710703	800	0.13	−0.92	0.11	0.33	3,523	0.11	0.31	0.08	0.41
rs62332588	800	0.39	−0.22	0.59	0.08	3,523	0.38	0.17	0.13	0.32
rs74682426	800	0.14	−0.85	0.14	0.30	3,523	0.12	0.29	0.10	0.38
rs62332591	800	0.46	−0.31	0.42	0.12	3,523	0.43	0.30	8.36×10^{-3}	0.75
rs56158232	800	0.24	−0.71	0.14	0.32	3,523	0.23	0.18	0.17	0.28
rs56023411	800	0.24	−0.71	0.14	0.32	3,523	0.23	0.15	0.25	0.21
rs2853672	800	0.50	−0.46	0.21	0.20	3,523	0.49	0.38	5.61×10^{-4}	0.93
rs2736098	800	0.35	−0.13	0.71	0.06	3,523	0.37	0.31	6.66×10^{-3}	0.76
rs2853669	800	0.36	−0.04	0.91	0.05	3,523	0.38	0.28	0.01	0.68
rs7712562	800	0.14	−0.86	0.12	0.31	3,523	0.12	0.27	0.12	0.35
rs2735940	800	0.50	−0.47	0.21	0.21	3,523	0.49	0.39	4.06×10^{-4}	0.94
rs2736109	800	0.33	−0.26	0.48	0.09	3,523	0.31	0.31	9.10×10^{-3}	0.73
rs6554754	800	0.14	−1.09	0.06	0.45	3,523	0.12	0.27	0.12	0.34
rs2736108	800	0.30	−0.35	0.37	0.12	3,523	0.29	0.21	0.09	0.40
rs2736107	800	0.28	−0.31	0.43	0.11	3,523	0.26	0.25	0.05	0.49
rs7449190	800	0.17	−0.89	0.09	0.37	3,523	0.14	0.22	0.16	0.28
rs13174814	800	0.48	0.51	0.20	0.24	3,523	0.48	−0.29	9.07×10^{-3}	0.73
rs4975612	800	0.47	0.48	0.23	0.22	3,523	0.48	−0.25	0.02	0.61
rs10462706	800	0.39	0.40	0.33	0.16	3,523	0.38	−0.23	0.05	0.50

Abbreviations: IEAA, intrinsic epigenetic age acceleration; LTL, leukocyte telomere length; MAF, minor allele frequency; TERT, telomerase reverse transcriptase.

Supplementary Table S10. Trait Variances Captured by Instrument SNPs and Power of Detecting the Causal Effect for MR Analysis

Exposure	$\sigma^2(x)$	$\sigma^2(y)$	$R^2(xz)$	β_{OLS}	β_{yx}	n	Power
LTL (public)	0.06	1	0.03	−0.015	0.06	38,000	0.08
IEAA (public)	1	1	0.17	0.001	−0.03	34,000	0.63

Abbreviations: IEAA, intrinsic epigenetic age acceleration; LTL, leukocyte telomere length; MR, Mendelian randomization.

Supplementary Table S11. Two-Sample–Based MR Results for TL, IEAA, and Nonfacial SL

Exposure Outcome	Method	Beta	SE	*P*-Value
TL_IEAA	pleiotropy	0.66	0.05	1.93×10^{-4}
	Maximum likelihood	24.98	2.92	1.12×10^{-17}
	MR Egger	−2.15	1.24	0.16
	MR Egger (bootstrap)	1.62	1.14	0.07
	Simple median	64.55	11.81	4.57×10^{-8}
	Weighted median	6.84	1.17	5.48×10^{-9}
	Penalized weighted median	6.44	1.23	1.72×10^{-7}
	Inverse variance weighted	8.88	5.39	0.10
	Inverse variance weighted (multiplicative random effects)	8.88	5.39	0.10
	Inverse variance weighted (fixed effects)	8.88	0.92	3.11×10^{-22}
	Simple mode	67.14	16.59	0.01
	Weighted mode	6.21	1.19	3.42×10^{-3}
	Weighted mode (NOME)	6.21	0.92	1.07×10^{-3}
	Simple mode (NOME)	67.14	6.41	1.37×10^{-4}
	Unweighted regression	10.57	12.33	0.39
TL_SL	pleiotropy	0.00	0.02	0.89
	Maximum likelihood	0.00	0.15	0.97
	MR Egger	−0.04	0.35	0.91
	MR Egger (bootstrap)	−0.07	0.29	0.39
	Simple median	0.15	0.23	0.52
	Weighted median	0.07	0.18	0.71
	Penalized weighted median	0.07	0.18	0.71
	Inverse variance weighted	0.00	0.15	0.97
	Inverse variance weighted (random effects)	0.00	0.15	0.97
	Inverse variance weighted (fixed effects)	0.00	0.15	0.97
	Simple mode	0.25	0.24	0.34
	Weighted mode	0.08	0.21	0.70
	Weighted mode (NOME)	0.08	0.21	0.70
	Simple mode (NOME)	0.25	0.24	0.35
	Unweighted regression	0.02	6.18	1.00
IEAA_SL	pleiotropy	0.06	0.04	0.20
	Maximum likelihood	−0.03	0.01	0.02
	MR Egger	−0.15	0.09	0.13
	MR Egger (bootstrap)	−0.10	0.06	0.03
	Simple median	−0.01	0.02	0.69
	Weighted median	−0.01	0.02	0.55
	Penalized weighted median	−0.01	0.02	0.62
	Inverse variance weighted	−0.03	0.01	0.02
	Inverse variance weighted (random effects)	−0.03	0.01	3.61×10^{-4}
	Inverse variance weighted (fixed effects)	−0.03	0.01	0.02
	Simple mode	−0.01	0.03	0.85
	Weighted mode	−0.01	0.03	0.84
	Weighted mode (NOME)	−0.01	0.03	0.85
	Simple mode (NOME)	−0.01	0.03	0.83
	Unweighted regression	−0.02	0.45	0.96

Abbreviations: IEAA, intrinsic epigenetic age acceleration; MR, Mendelian randomization; NOME, no measurement error; SE, standard error; SL, solar lentigines; TL, telomere length.

Supplementary Table S12. Mendelian Randomization Results Using CAUSE Method

		P-Value from CAUSE		
Exposure	**Outcome**	**Sharing Versus Null**	**Causal Versus Null**	**Causal Versus Sharing**
BCC	SL	0.89	0.85	0.73
IEAA	SL	0.96	0.93	0.87
SK	SL	0.4	0.23	0.18
LTL	SL	0.86	0.8	0.72
SL	BCC	0.93	0.75	0.62
SL	IEAA	0.96	0.93	0.87
SL	SK	0.46	0.32	0.27
SL	LTL	0.43	0.64	1

Abbreviations: BCC, basal cell carcinoma; IEAA, intrinsic epigenetic age acceleration; LTL, leukocyte telomere length; SK, seborrhoeic keratosis; SL, solar lentigines.

Supplementary Table S13. The Association between Non-facial SL–Related SNPs and Facial SL Adjusted for Relatedness by GCTA (fastGWA)

				Meta-Analysis			TZL			NSPT			SALIA		
CHR	BP	SNP	A1	Beta	SE	*P*-Value	Beta	SE	*P*-Value	Beta	SE	*P*-Value	Beta	SE	*P*-Value
5	1276050	rs113136187	t	0.05	0.02	0.01	0.05	0.03	0.10	0.04	0.02	0.05	0.13	0.09	0.16
5	1279790	rs10069690	t	−0.06	0.02	7.70×10^{-4}	−0.09	0.03	3.52×10^{-3}	−0.04	0.02	0.06	−0.07	0.08	0.36
5	1279964	rs10054203	c	−0.03	0.01	0.01	−0.04	0.02	0.09	−0.03	0.02	0.10	−0.07	0.07	0.30
5	1280028	rs2242652	a	−0.05	0.02	3.81×10^{-3}	−0.07	0.03	0.02	−0.03	0.02	0.14	−0.14	0.09	0.12
5	1280128	rs7734992	t	0.04	0.01	1.19×10^{-3}	0.05	0.02	0.05	0.04	0.02	0.03	0.14	0.07	0.04
5	1280830	rs4975538	c	−0.02	0.01	0.08	−0.04	0.02	0.07	−0.01	0.02	0.57	−0.09	0.07	0.19
5	1280938	rs6897196	a	0.03	0.01	0.03	0.05	0.02	0.05	0.02	0.02	0.31	0.09	0.07	0.20
5	1282319	rs7726159	a	−0.04	0.01	0.01	−0.05	0.02	0.02	−0.02	0.02	0.17	−0.06	0.07	0.37
5	1282414	rs7725218	a	−0.04	0.01	0.01	−0.06	0.02	0.01	−0.02	0.02	0.16	−0.07	0.07	0.34
5	1283312	rs7713218	a	−0.04	0.01	0.01	−0.06	0.02	0.01	−0.03	0.02	0.12	−0.01	0.07	0.85
5	1283486	rs7717443	t	−0.03	0.01	0.01	−0.05	0.02	0.02	−0.03	0.02	0.12	−0.01	0.07	0.84
5	1283755	rs72709458	t	−0.05	0.02	2.23×10^{-3}	−0.09	0.03	2.27×10^{-3}	−0.03	0.02	0.23	−0.14	0.08	0.10
5	1284135	rs4449583	t	−0.04	0.01	0.01	−0.05	0.02	0.02	−0.02	0.02	0.15	−0.07	0.07	0.36
5	1285162	rs10866498	t	0.04	0.01	2.61×10^{-3}	0.06	0.02	0.01	0.03	0.02	0.06	0.04	0.07	0.58
5	1285974	rs7705526	a	−0.04	0.01	0.01	−0.05	0.02	0.03	−0.02	0.02	0.20	−0.18	0.07	0.01
5	1286516	rs2736100	a	0.04	0.01	7.57×10^{-4}	0.06	0.02	0.01	0.02	0.02	0.16	0.23	0.07	7.87×10^{-4}
5	1287194	rs2853677	a	0.04	0.01	3.64×10^{-3}	0.05	0.02	0.03	0.02	0.02	0.16	0.20	0.07	4.17×10^{-3}
5	1287340	rs2736099	a	−0.05	0.01	1.43×10^{-4}	−0.07	0.02	3.39×10^{-3}	−0.03	0.02	0.06	−0.21	0.07	1.39×10^{-3}
5	1287505	rs7710703	t	−0.08	0.02	1.35×10^{-4}	−0.06	0.04	0.15	−0.08	0.03	4.64×10^{-3}	−0.37	0.10	3.19×10^{-4}
5	1288547	rs2853676	t	−0.09	0.02	2.54×10^{-7}	−0.10	0.03	8.26×10^{-4}	−0.07	0.02	2.03×10^{-3}	−0.27	0.08	2.66×10^{-4}
5	1289880	rs62332588	t	−0.04	0.01	1.12×10^{-3}	−0.07	0.02	0.01	−0.03	0.02	0.13	−0.16	0.07	0.01
5	1289975	rs74682426	a	−0.08	0.02	9.82×10^{-5}	−0.05	0.04	0.21	−0.08	0.03	1.27×10^{-3}	−0.29	0.10	3.45×10^{-3}
5	1290319	rs62332591	t	−0.06	0.01	1.73×10^{-6}	−0.08	0.02	1.06×10^{-3}	−0.05	0.02	4.07×10^{-3}	−0.21	0.07	1.51×10^{-3}
5	1291735	rs56158232	a	0.02	0.02	0.17	0.01	0.03	0.61	0.02	0.02	0.35	0.15	0.08	0.08
5	1291740	rs56023411	t	0.03	0.02	0.06	0.01	0.03	0.61	0.03	0.02	0.11	0.15	0.08	0.08
5	1292983	rs2853672	a	0.07	0.01	4.42×10^{-7}	0.07	0.02	1.18×10^{-3}	0.05	0.02	1.30×10^{-3}	0.22	0.07	8.88×10^{-4}
5	1294086	rs2736098	t	−0.04	0.01	1.71×10^{-3}	−0.07	0.02	2.30×10^{-3}	−0.02	0.02	0.18	−0.14	0.08	0.06
5	1295349	rs2853669	a	0.04	0.01	4.90×10^{-3}	0.07	0.02	2.91×10^{-3}	0.02	0.02	0.26	0.09	0.07	0.22
5	1296072	rs7712562	a	−0.09	0.02	5.88×10^{-5}	−0.05	0.04	0.23	−0.09	0.03	6.60×10^{-4}	−0.30	0.10	3.20×10^{-3}
5	1296486	rs2735940	a	−0.06	0.01	8.63×10^{-7}	−0.06	0.02	4.71×10^{-3}	−0.05	0.02	8.24×10^{-4}	−0.23	0.07	7.60×10^{-4}
5	1296759	rs2736109	t	−0.04	0.01	4.81×10^{-3}	−0.07	0.02	2.77×10^{-3}	−0.02	0.02	0.19	−0.02	0.07	0.79
5	1297258	rs6554754	t	−0.07	0.02	6.48×10^{-4}	−0.04	0.04	0.34	−0.08	0.03	3.11×10^{-3}	−0.28	0.11	0.01
5	1297488	rs2736108	t	−0.05	0.01	3.42×10^{-4}	−0.08	0.02	1.05×10^{-3}	−0.03	0.02	0.07	−0.10	0.07	0.16
5	1297854	rs2736107	t	−0.05	0.01	1.44×10^{-3}	−0.06	0.03	0.01	−0.04	0.02	0.05	−0.09	0.07	0.22
5	1297918	rs7449190	t	−0.08	0.02	3.09×10^{-5}	−0.07	0.03	0.04	−0.07	0.02	2.48×10^{-3}	−0.30	0.10	3.20×10^{-3}
5	1299859	rs13174814	c	0.02	0.01	0.07	−0.01	0.02	0.53	0.04	0.02	0.03	0.18	0.08	0.02
5	1299862	rs13174919	c	0.03	0.01	0.02	0.00	0.02	0.87	0.04	0.02	0.01	0.15	0.08	0.05
5	1300310	rs4975612	t	0.02	0.01	0.17	0.00	0.02	0.83	0.02	0.02	0.16	0.19	0.08	0.02
5	1300429	rs2735946	t	0.00	0.02	0.86	0.08	0.04	0.05	−0.02	0.03	0.40	−0.14	0.07	0.05
5	1343794	rs10462706	t	0.03	0.01	0.05	−0.01	0.02	0.63	0.04	0.02	0.01	0.15	0.09	0.10
15	28197037	rs1800414	t	−0.03	0.01	0.01	−0.03	0.02	0.18	−0.03	0.02	0.04	−0.26	0.71	0.72

Abbreviations: BP, base position; CHR, chromosome; GCTA, Genome-wide Complex Trait Analysis; NSPT, National Survey of Physical Traits; SE, standard error; TZL, Taizhou longitudinal cohort.

Supplementary Table S14. Environmental Factors Association with Facial and Non-facial SL in Discovery Dataset

	Non-facial SL				Facial SL			
Environmental Factor	**Beta**	**SE**	***P*-Value**	**r^2, %**	**Beta**	**SE**	***P*-Value**	**R^2, %**
Skincare frequency	0.01	0.03	0.83	0.00	**−0.16**	**0.04**	**1.54×10^{-5}**	**0.69**
Sunshade habit	−0.05	0.03	0.14	0.08	0	0.04	0.97	0.00
Mean sunexposed time	**0.04**	**0.01**	**1.95×10^{-5}**	**0.67**	**−0.05**	**0.01**	**2.90×10^{-5}**	**0.65**
Meat eating frequency	0.01	0.02	0.51	0.02	**0.06**	**0.02**	**6.51×10^{-4}**	**0.43**
Fruit-eating frequency	**0.05**	**0.02**	**1.63×10^{-3}**	**0.37**	0	0.02	0.98	0.00
Egg eating frequency	**0.06**	**0.02**	**1.65×10^{-4}**	**0.52**	0	0.02	0.79	0.00
Bean eating frequency	0.04	0.02	0.03	0.19	0.05	0.02	6.42×10^{-3}	0.28
Milk drinking frequency	**0.07**	**0.02**	**1.94×10^{-4}**	**0.51**	−0.05	0.02	7.59×10^{-3}	0.26
Ventilator using	**0.17**	**0.05**	**4.95×10^{-4}**	**0.45**	**−0.24**	**0.05**	**1.06×10^{-5}**	**0.72**
Urban living	0.1	0.04	1.21×10^{-2}	0.23	**−0.46**	**0.04**	**4.87×10^{-24}**	**3.72**
Airconditioner use	**0.13**	**0.03**	**2.48×10^{-4}**	**0.50**	−0.07	0.04	0.08	0.11
Cook straw	0.13	0.05	1.07×10^{-2}	0.24	**−0.31**	**0.05**	**2.01×10^{-8}**	**1.16**
Education	**0.1**	**0.01**	**1.04×10^{-12}**	**1.87**	−0.04	0.01	1.21×10^{-2}	0.23
Annual income	0.04	0.02	7.58×10^{-3}	0.26	**−0.08**	**0.02**	**9.80×10^{-7}**	**0.88**

Abbreviations: SE, standard error; SL, solar lentigines.
Boldfaces indicate significant associations between environmental factors and nonfacial SL at a threshold of $0.05/14/2 = 1.79 \times 10^{-3}$.

Supplementary Table S15. The Association between TERT SNP rs2853672 and Facial and Non-facial SLs in High-Dose and Low-Dose Sun Exposure Groups in TZL and NSPT

Cohort	**Trait**	**Exposure**	**Sample Size**	**Beta**	**SE**	***P*-Value**
TZL	Non-facial SL	High exposure	1,534	−0.26	0.03	2.21×10^{-18}
		Low exposure	1,005	−0.17	0.03	6.18×10^{-6}
	Facial SL	High exposure	1,534	−0.10	0.03	0.001
		Low exposure	1,005	−0.06	0.04	0.13
NSPT	Non-facial SL	High exposure	1,567	−0.20	0.03	3.20×10^{-13}
		Low exposure	1,339	−0.12	0.02	6.77×10^{-7}
	Facial SL	High exposure	1,567	−0.08	0.02	8.60×10^{-4}
		Low exposure	1,339	−0.02	0.02	0.29

Abbreviations: SE, standard error; NSPT, National Survey of Physical Traits; SL, solar lentigines; TERT, telomerase reverse transcriptase; TZL, Taizhou longitudinal cohort.

Supplementary Table S16. Heterogeneity (I^2, Q) Measures of Non-facial SL–Associated SNPs Adjusted for Relatedness by GCTA (fastGWA)

			Nonfacial SL			Facial SL		
CHR	BP	SNP	I^2	Q	P_{HET}	I^2	Q	P_{HET}
5	1276050	rs113136187	0.00	1.63	0.44	0.00	0.88	0.64
5	1279790	rs10069690	0.00	0.70	0.71	0.00	1.45	0.49
5	1279964	rs10054203	41.50	3.42	0.18	0.00	0.47	0.79
5	1280028	rs2242652	0.00	1.67	0.43	4.40	2.09	0.35
5	1280128	rs7734992	39.50	3.31	0.19	13.70	2.32	0.31
5	1280830	rs4975538	13.90	2.32	0.31	13.00	2.30	0.32
5	1280938	rs6897196	4.60	2.10	0.35	0.00	1.70	0.43
5	1282319	rs7726159	0.00	1.73	0.42	0.00	1.31	0.52
5	1282414	rs7725218	0.00	1.83	0.40	0.00	1.48	0.48
5	1283312	rs7713218	14.80	2.35	0.31	0.00	1.31	0.52
5	1283486	rs7717443	9.70	2.22	0.33	0.00	1.02	0.60
5	1283755	rs72709458	54.40	4.38	0.11	49.70	3.98	0.14
5	1284135	rs4449583	19.40	2.48	0.29	0.00	1.32	0.52
5	1285162	rs10866498	32.40	2.96	0.23	0.00	0.78	0.68
5	1285974	rs7705526	53.20	4.28	0.12	58.70	4.84	0.09
5	1286516	rs2736100	74.10	7.71	0.02	79.20	9.60	0.01
5	1287194	rs2853677	68.50	6.35	0.04	67.90	6.23	0.04
5	1287340	rs2736099	70.00	6.67	0.04	74.20	7.75	0.02
5	1287505	rs7710703	73.30	7.49	0.02	75.90	8.31	0.02
5	1288547	rs2853676	74.70	7.89	0.02	72.30	7.23	0.03
5	1289880	rs62332588	68.80	6.42	0.04	62.10	5.28	0.07
5	1289975	rs74682426	73.20	7.46	0.02	61.50	5.20	0.07
5	1290319	rs62332591	74.20	7.75	0.02	66.70	6.00	0.05
5	1291735	rs56158232	14.80	2.35	0.31	16.50	2.39	0.30
5	1291740	rs56023411	44.50	3.60	0.17	13.40	2.31	0.32
5	**1292983**	**rs2853672**	**77.20**	**8.77**	**0.01**	**67.90**	**6.22**	**0.04**
5	1294086	rs2736098	56.30	4.58	0.10	56.70	4.62	0.10
5	1295349	rs2853669	55.10	4.46	0.11	45.10	3.64	0.16
5	1296072	rs7712562	56.20	4.57	0.10	63.30	5.45	0.07
5	1296486	rs2735940	71.20	6.93	0.03	67.30	6.11	0.05
5	1296759	rs2736109	0.00	1.80	0.41	27.20	2.75	0.25
5	1297258	rs6554754	40.70	3.37	0.19	55.00	4.45	0.11
5	1297488	rs2736108	0.00	0.88	0.65	32.80	2.98	0.23
5	1297854	rs2736107	0.00	0.57	0.75	0.00	0.99	0.61
5	1297918	rs7449190	55.20	4.47	0.11	57.80	4.74	0.09
5	1299859	rs13174814	0.00	1.94	0.38	72.70	7.32	0.03
5	1299862	rs13174919	0.00	1.18	0.55	60.50	5.06	0.08
5	1300310	rs4975612	10.20	2.23	0.33	63.70	5.52	0.06
5	1300429	rs2735946	0.00	0.47	0.79	76.00	8.32	0.02
5	1343794	rs10462706	0.00	1.05	0.59	61.60	5.21	0.07
15	28197037	rs1800414	0.00	1.63	0.44	0.00	0.12	0.94

Abbreviations: BP, base position; CHR, chromosome; GCTA, Genome-wide Complex Trait Analysis; SL, solar lentigines.
Boldfaces indicate the top SNP associated with nonfacial SL in our study.

Supplementary Table S17. SNPs Ranked by Putative Functional Significance Evaluated according to IW Scoring

SNP	IW Score	SNP	IW Score
rs2853669	3.0113	rs2853676	−2.3279
rs2735940	1.8546	rs74682426	−2.5745
rs2736098	1.7305	rs56158232	−2.7215
rs7712562	0.0163	rs6554754	−2.8173
rs56023411	−1.8673	rs62332588	−2.9164
rs62332591	−2.0439	rs7449190	−3.0832

Abbreviation: IW, Integrative Weighted.
Boldfaces indicate SNPs selected on the basis of IW scoring method.

Supplementary Table S18. Instrument SNPs for Exposure LTL

CHR	SNP	BP	Effect Allele	Beta/OR	*P*-Value
5	rs10069690	1279790	T	1.009	0.013
5	rs2242652	1280028	A	1.009	0.016
5	rs7734992	1280128	C	1.019	2.23×10^{-9}
5	rs11278847	1280940	G	1.023	1.62×10^{-11}
5	rs7726159	1282319	A	1.024	4.52×10^{-13}
5	rs7725218	1282414	A	1.021	1.10×10^{-10}
5	rs72709458	1283755	T	1.012	0.001
5	rs4449583	1284135	T	1.025	1.93×10^{-13}
5	rs7705526	1285974	A	1.026	2.32×10^{-14}
5	rs2736100	1286516	C	0.078[a]	4.38×10^{-19}
5	rs2736098	1294086	T	1.017	1.35×10^{-6}
5	rs2853669	1295349	G	1.016	2.95×10^{-6}
5	rs3215401	1296255	AAG	1.016	1.63×10^{-6}
5	rs10548207	1297077	A	1.016	7.13×10^{-6}
5	rs2736108	1297488	T	1.017	5.81×10^{-7}
5	rs2736107	1297854	T	1.015	8.33×10^{-7}

Abbreviations: BP, base position; CHR, chromosome; LTL, leukocyte telomere length.

Supplementary Table S19. Instrument SNPs for IEAA

CHR	BP	SNP	Beta	SE	Effect Allele	Other Allele	*P*-Value
3	160025238	rs6791056	0.39	0.07	A	G	1.51×10^{-8}
3	160036076	rs7620828	0.39	0.07	C	T	9.67×10^{-9}
3	160047306	rs869467	0.39	0.07	C	T	9.62×10^{-9}
3	160077943	rs7355951	0.40	0.07	G	C	4.84×10^{-9}
3	160123373	rs55992947	0.39	0.07	G	A	5.76×10^{-9}
3	160142618	rs11718121	0.4008	0.07	C	A	3.35×10^{-9}
3	160159921	rs11706810	0.41	0.07	C	T	1.63×10^{-9}
3	160191236	rs3851365	0.40	0.07	A	C	4.19×10^{-9}
3	160226575	rs4680591	0.40	0.07	C	T	3.53×10^{-9}
3	160258869	rs56156703	0.38	0.07	T	A	9.30×10^{-9}
3	160272388	rs4679654	0.41	0.07	T	A	2.13×10^{-9}
5	1287340	rs2736099	0.63	0.09	A	G	1.29×10^{-12}
6	18104322	rs6920558	0.51	0.07	A	G	2.62×10^{-13}
6	18117868	rs11758925	0.53	0.07	A	G	1.16×10^{-13}
6	18149668	rs3930695	0.48	0.08	G	T	1.40×10^{-9}
6	18174085	rs138907444	−0.64	0.10	T	C	9.74×10^{-10}
6	18186591	rs72840608	−0.59	0.10	G	A	3.87×10^{-9}
6	25585844	rs6935612	−0.42	0.07	C	T	6.27×10^{-9}
6	25608374	rs3804106	−0.41	0.07	A	G	6.65×10^{-9}
6	25624800	rs73397619	−0.46	0.07	C	T	2.30×10^{-10}
6	25642577	rs10447389	−0.45	0.07	A	G	5.19×10^{-10}
6	25661887	rs2072847	−0.46	0.07	T	A	3.81×10^{-10}
17	53084650	rs12051894	−0.46	0.08	A	G	1.82×10^{-8}
17	53102367	rs78781855	−0.48	0.08	G	T	5.59×10^{-9}
17	53121020	rs17818142	−0.47	0.08	G	A	8.63×10^{-9}
17	53145604	rs17818238	−0.46	0.08	A	G	1.67×10^{-8}
17	53167452	rs1548908	−0.47	0.08	T	C	9.96×10^{-9}

Abbreviations: BP, base position; CHR, chromosome; IEAA, intrinsic epigenetic age acceleration; SE, standard error.

Supplementary Table S20. The Association between rs2853672 and One Single Composite SL Phenotype in TZL and NSPT

Data	CHR	BP	SNP	Beta	SE	t-Value	*P*-Value
TZL	5	1292983	rs2853672	−0.09	0.02	−4.86	1.21×10^{-6}
NSPT	5	1292983	rs2853672	−0.08	0.02	−4.92	8.99×10^{-7}

Abbreviations: BP, base position; CHR, chromosome; NSPT, National Survey of Physical Traits; SE, standard error; SL, solar lentigines; TZL, Taizhou longitudinal cohort.

Supplementary Table S21. Significant SNPs Associated with Non-facial SL in Samples with IBD < 0.1875

				Meta			Discovery 1 (TZL)			Discovery 2 (NSPT)			Replication (SALIA)		
CHR	BP	SNP	A1	Beta	SE	*P*-Value	Beta	SE	*P*-Value	Beta	SE	*P*-Value	Beta	SE	*P*-Value
5	1276050	rs113136187	t	0.11	0.02	3.76×10^{-9}	0.14	0.03	6.69×10^{-7}	0.09	0.03	1.10×10^{-3}	0.19	0.13	0.15
5	1279790	rs10069690	t	−0.12	0.02	1.12×10^{-9}	−0.14	0.03	3.88×10^{-7}	−0.10	0.03	4.75×10^{-4}	−0.11	0.11	0.32
5	1279964	rs10054203	c	−0.09	0.01	1.29×10^{-9}	−0.12	0.02	9.27×10^{-8}	−0.07	0.02	1.14×10^{-3}	−0.11	0.10	0.27
5	1280028	rs2242652	a	−0.12	0.02	2.46×10^{-10}	−0.16	0.03	5.36×10^{-8}	−0.09	0.03	8.18×10^{-4}	−0.20	0.13	0.11
5	1280128	rs7734992	t	0.10	0.02	3.30×10^{-11}	0.12	0.02	9.93×10^{-8}	0.08	0.02	1.45×10^{-4}	0.21	0.10	0.03
5	1280830	rs4975538	c	−0.10	0.02	8.26×10^{-11}	−0.12	0.02	1.09×10^{-7}	−0.08	0.02	1.43×10^{-4}	−0.13	0.10	0.18
5	1280938	rs6897196	a	0.10	0.02	4.32×10^{-11}	0.12	0.02	6.56×10^{-8}	0.08	0.02	1.15×10^{-4}	0.13	0.10	0.18
5	1282319	rs7726159	a	−0.10	0.02	8.55×10^{-12}	−0.13	0.02	1.32×10^{-8}	−0.08	0.02	6.38×10^{-5}	−0.09	0.10	0.36
5	1283312	rs7713218	a	−0.11	0.01	2.40×10^{-14}	−0.14	0.02	4.74×10^{-10}	−0.10	0.02	2.04×10^{-6}	−0.02	0.10	0.83
5	1283486	rs7717443	t	−0.11	0.01	3.14×10^{-14}	−0.14	0.02	7.18×10^{-10}	−0.10	0.02	1.94×10^{-6}	−0.02	0.10	0.83
5	1283755	rs72709458	t	−0.13	0.02	3.86×10^{-12}	−0.18	0.03	1.57×10^{-10}	−0.09	0.03	9.92×10^{-4}	−0.20	0.12	0.09
5	1284135	rs4449583	t	−0.10	0.02	6.26×10^{-12}	−0.13	0.02	4.53×10^{-9}	−0.08	0.02	1.01×10^{-4}	−0.10	0.10	0.34
5	1285162	rs10866498	t	0.12	0.01	5.73×10^{-15}	0.15	0.02	5.31×10^{-11}	0.09	0.02	3.60×10^{-6}	0.05	0.10	0.58
5	1285974	rs7705526	a	−0.11	0.02	3.50×10^{-13}	−0.13	0.02	2.29×10^{-9}	−0.08	0.02	5.54×10^{-5}	−0.25	0.10	0.01
5	1286516	rs2736100	a	0.14	0.01	5.76×10^{-20}	0.16	0.02	5.54×10^{-13}	0.11	0.02	1.54×10^{-7}	0.33	0.10	5.76×10^{-4}
5	1287194	rs2853677	a	0.16	0.02	1.50×10^{-26}	0.19	0.02	1.46×10^{-16}	0.13	0.02	9.42×10^{-11}	0.28	0.10	3.91×10^{-3}
5	1287505	rs7710703	t	−0.23	0.02	3.99×10^{-21}	−0.26	0.04	2.14×10^{-12}	−0.19	0.03	8.33×10^{-9}	−0.53	0.14	2.17×10^{-4}
5	1289880	rs62332588	t	−0.18	0.01	5.37×10^{-33}	−0.22	0.02	4.76×10^{-22}	−0.14	0.02	1.68×10^{-12}	−0.24	0.09	0.01
5	1289975	rs74682426	a	−0.22	0.02	2.23×10^{-19}	−0.27	0.04	2.44×10^{-13}	−0.16	0.03	3.83×10^{-7}	−0.42	0.14	2.54×10^{-3}
5	1290319	rs62332591	t	−0.18	0.01	3.63×10^{-35}	−0.21	0.02	5.99×10^{-22}	−0.15	0.02	1.03×10^{-13}	−0.31	0.09	8.44×10^{-4}
5	1291735	rs56158232	a	0.16	0.02	1.52×10^{-19}	0.20	0.03	1.02×10^{-12}	0.13	0.02	2.70×10^{-8}	0.23	0.12	0.05
5	1291740	rs56023411	t	0.15	0.02	1.88×10^{-17}	0.20	0.03	1.02×10^{-12}	0.12	0.02	1.24×10^{-6}	0.23	0.12	0.05
5	**1292983**	**rs2853672**	**a**	**0.20**	**0.01**	$\mathbf{5.66 \times 10^{-42}}$	**0.23**	**0.02**	$\mathbf{2.01 \times 10^{-25}}$	**0.17**	**0.02**	$\mathbf{7.62 \times 10^{-17}}$	**0.32**	**0.09**	$\mathbf{7.41 \times 10^{-4}}$
5	1294086	rs2736098	t	−0.13	0.02	5.78×10^{-17}	−0.15	0.02	6.98×10^{-11}	−0.11	0.02	2.24×10^{-7}	−0.20	0.11	0.06
5	1295349	rs2853669	a	0.12	0.02	3.09×10^{-16}	0.15	0.02	6.59×10^{-11}	0.10	0.02	5.01×10^{-7}	0.13	0.10	0.22
5	1296072	rs7712562	a	−0.20	0.02	4.00×10^{-17}	−0.23	0.04	2.57×10^{-10}	−0.17	0.03	2.67×10^{-7}	−0.43	0.14	2.39×10^{-3}
5	1296486	rs2735940	a	−0.19	0.01	2.48×10^{-39}	−0.22	0.02	5.40×10^{-23}	−0.16	0.02	1.94×10^{-16}	−0.32	0.09	6.78×10^{-4}
5	1296759	rs2736109	t	−0.09	0.02	5.28×10^{-9}	−0.11	0.02	6.16×10^{-6}	−0.08	0.02	1.15×10^{-4}	−0.03	0.10	0.77
5	1297258	rs6554754	t	−0.20	0.02	1.65×10^{-16}	−0.23	0.04	8.26×10^{-10}	−0.17	0.03	1.95×10^{-7}	−0.41	0.15	8.38×10^{-3}
5	1297488	rs2736108	t	−0.10	0.02	2.18×10^{-10}	−0.11	0.02	8.62×10^{-6}	−0.10	0.02	1.23×10^{-5}	−0.15	0.10	0.16
5	1297854	rs2736107	t	−0.09	0.02	1.17×10^{-8}	−0.10	0.02	5.27×10^{-5}	−0.09	0.02	9.64×10^{-5}	−0.13	0.10	0.23
5	1297918	rs7449190	t	−0.18	0.02	1.21×10^{-16}	−0.20	0.03	9.09×10^{-10}	−0.15	0.03	2.38×10^{-7}	−0.43	0.14	2.39×10^{-3}
5	1299859	rs13174814	c	0.10	0.01	1.51×10^{-11}	0.09	0.02	3.27×10^{-5}	0.10	0.02	5.00×10^{-7}	0.25	0.11	0.02
5	1300310	rs4975612	t	0.10	0.01	2.85×10^{-12}	0.09	0.02	3.35×10^{-5}	0.11	0.02	8.18×10^{-8}	0.26	0.11	0.02
5	1343794	rs10462706	t	0.09	0.02	1.22×10^{-8}	0.09	0.02	7.37×10^{-5}	0.08	0.02	8.59×10^{-5}	0.20	0.13	0.11
15	28196145	rs76930569	t	0.08	0.02	2.45×10^{-8}	−0.11	0.02	2.78×10^{-6}	−0.07	0.02	9.05×10^{-4}	0.32	1.00	0.75
15	28197037	rs1800414	t	−0.09	0.02	1.94×10^{-8}	−0.11	0.02	3.05×10^{-6}	−0.07	0.02	6.97×10^{-4}	−0.32	1.00	0.75

Abbreviations: BP, base postion; CHR, chromosome; IBD, identity by descent; NSPT, National Survey of Physical Traits; SE, standard error; SL, solar lentigines; TZL, Taizhou longitudinal cohort.
Boldfaces indicate the top SNP associated with nonfacial SL in our study.

Supplementary Table S22. Replication of Candidate SNPs Detected in Previous Four SL-Based GWASs in Samples with IBD < 0.1875

						Replication in Han Chinese (TZL + NSPT)				
							Facial SL		Nonfacial SL	
Study	CHR	Gene	SNP	EAF (EA)[1]	Beta/Log (OR)	EAF	Beta	*P*-Value	Beta	*P*-Value
Dutch GWAS (Jacobs et al., 2015) (n = 2,844)	6	*IRF4*	rs12203592	0.09 (T)	0.44	<0.01	—	—	—	—
	9	*BNC2*	rs62543565	0.37 (C)	−0.15	0.68	0.01	0.35	−0.02	0.28
	16	*MC1R*	rs35063026	0.07 (T)	0.33	<0.01	—	—	—	—
	20	*RALY/ASIP*	rs6059655	0.08 (A)	0.3	<0.01	—	—	—	—
French GWAS (Laville et al., 2016) (n = 502)	6	*6p21 intergenic*	rs9350204	0.15 (C)	—	0.37	0.002	0.91	0.02	0.27
			rs9358294	0.15 (G)	—	0.36	0.002	0.91	0.02	0.28
	6	*HLC-C* (near gene)	rs2853949	0.14 (A)	—	0.01	−0.05	0.61	−0.09	0.35
	6	*USP8P1*	rs2844614	0.14 (A)	—	0.01	−0.05	0.61	−0.09	0.35
			rs2844613	0.14 (T)	—	0.01	−0.05	0.61	−0.09	0.35
			rs2524069	0.13 (T)	—	0.02	−0.03	0.72	−0.12	0.11
			rs2853947	0.14 (T)	—	0.03	−0.06	0.16	−0.04	0.34
			rs2524067	0.14 (G)	—	0.03	−0.06	0.16	−0.04	0.34
			rs2524065	0.14 (C)	—	0.03	−0.06	0.16	−0.04	0.34
Japanese GWAS (Endo et al., 2018) (n = 11,311)	**5**	*PPARGC1B*	**rs251468**	**0.18 (T)**	**−0.11**	**0.21**	**−0.06**	**5.81×10^{-4}**	−0.06	1.77×10^{-3}
	9	*BNC2*	rs10810635	0.47 (T)	−0.12	0.72	−0.04	0.01	−0.03	0.06
	10	*RAB11FIP2*	**rs61866017**	**0.16 (T)**	**−0.11**	**0.12**	−0.03	0.22	**−0.08**	**1.22×10^{-3}**
			rs35563099	**0.09 (T)**	**−0.11**	**0.1**	−0.03	0.18	**−0.10**	**1.24×10^{-4}**
			rs10444039	**0.09 (A)**	**−0.22**	**0.1**	−0.04	0.11	**−0.09**	**1.35×10^{-4}**
			rs10886142	0.49 (T)	0.08	0.45	0.02	0.21	0.01	0.51
			rs4752116	0.21 (T)	−0.09	0.21	−0.03	0.12	−0.04	0.02
	10	*HSPA12A*	**rs12259842**	**0.25 (T)**	**0.09**	**0.21**	0.04	0.02	**0.08**	**4.76×10^{-6}**
	17	*AKAP1/MSI2*	rs17833789	0.45 (C)	0.07	0.48	0.02	0.25	0.01	0.49
Korean GWAS (Shin et al., 2021) (n = 17,019)	2	*LINC01877*	rs12693889	0.50 (T)	0.6	0.45	0.02	0.16	0.03	0.04
	5	*PPARGC1B*	rs32579	0.30 (T)	−1.56	0.35	−0.04	0.01	−0.03	0.04
	9	*BNC2*	rs16935073	0.43 (C)	1.58	0.3	0.04	0.01	0.03	0.08
	9	*CDKN2B-AS1*	rs643319	0.36 (A)	−0.54	0.36	0.02	0.29	0.01	0.70
	10	*10q26*	**rs11198112**	**0.10 (T)**	**−2.3**	**0.1**	−0.04	0.11	**−0.09**	**2.60×10^{-4}**
	16	*MC1R*	rs2228479	0.14 (A)	1.55	0.21	0.03	0.32	0.06	0.03
	19	*MFSD12*	**rs2240751**	**0.34 (G)**	**−0.67**	**0.29**	**−0.08**	**3.45×10^{-6}**	−0.004	0.80

Abbreviations: CHR, chromosome; EAF, effect allele frequency; IBD, identity by descent; NSPT, National Survey of Physical Traits; SL, solar lentigines; TZL, Taizhou longitudinal cohort.

Boldface indicated SNP replicated in our study at a *P*-value threshold of $0.05/29 = 1.72 \times 10^{-3}$.

[1]EAF in the original GWAS; EA in the original GWAS.

Supplementary Table S23. The Association between Non-facial SL–Related SNPs and Facial SL in Samples with IBD < 0.1875

				Meta-Analysis			TZL			NSPT			SALIA		
CHR	BP	SNP	A1	Beta	SE	*P*-Value	Beta	SE	*P*-Value	Beta	SE	*P*-Value	Beta	SE	*P*-Value
5	1276050	rs113136187	t	0.04	0.02	0.02	0.05	0.03	0.07	0.03	0.02	0.19	0.13	0.09	0.16
5	1279790	rs10069690	t	−0.06	0.02	2.24×10^{-3}	−0.09	0.03	2.74×10^{-3}	−0.03	0.03	0.19	−0.07	0.08	0.36
5	1279964	rs10054203	c	−0.04	0.01	0.01	−0.04	0.02	0.08	−0.03	0.02	0.10	−0.07	0.07	0.30
5	1280028	rs2242652	a	−0.05	0.02	0.01	−0.07	0.03	0.02	−0.02	0.03	0.39	−0.14	0.09	0.12
5	1280128	rs7734992	t	0.05	0.01	9.15×10^{-4}	0.05	0.02	0.05	0.04	0.02	0.03	0.14	0.07	0.04
5	1280830	rs4975538	c	−0.03	0.01	0.05	−0.05	0.02	0.06	−0.01	0.02	0.50	−0.09	0.07	0.19
5	1280938	rs6897196	a	0.03	0.01	0.02	0.05	0.02	0.04	0.02	0.02	0.25	0.09	0.07	0.20
5	1282319	rs7726159	a	−0.04	0.01	0.01	−0.06	0.02	0.01	−0.02	0.02	0.25	−0.06	0.07	0.37
5	1283312	rs7713218	a	−0.04	0.01	0.01	−0.06	0.02	8.00×10^{-3}	−0.02	0.02	0.29	−0.01	0.07	0.85
5	1283486	rs7717443	t	−0.03	0.01	0.02	−0.06	0.02	0.01	−0.02	0.02	0.27	−0.01	0.07	0.84
5	1283755	rs72709458	t	−0.05	0.02	0.01	−0.09	0.03	2.05×10^{-3}	−0.01	0.02	0.71	−0.14	0.08	0.10
5	1284135	rs4449583	t	−0.04	0.01	0.01	−0.06	0.02	0.01	−0.02	0.02	0.27	−0.07	0.07	0.36
5	1285162	rs10866498	t	0.04	0.01	5.41×10^{-3}	0.06	0.02	7.85×10^{-3}	0.03	0.02	0.16	0.04	0.07	0.58
5	1285974	rs7705526	a	−0.04	0.01	9.69×10^{-3}	−0.06	0.02	0.02	−0.02	0.02	0.37	−0.18	0.07	0.01
5	1286516	rs2736100	a	0.05	0.01	1.31×10^{-3}	−0.07	0.02	3.79×10^{-3}	−0.02	0.02	0.32	0.23	0.07	7.87×10^{-4}
5	1287194	rs2853677	a	0.04	0.01	6.74×10^{-3}	−0.05	0.02	0.03	−0.02	0.02	0.31	0.20	0.07	4.17×10^{-3}
5	1287505	rs7710703	t	−**0**.08	0.02	6.09×10^{-4}	−0.06	0.04	0.11	−0.06	0.03	0.03	−0.37	0.10	3.19×10^{-4}
5	1289880	rs62332588	t	−0.05	0.01	1.32×10^{-3}	−0.07	0.02	2.84×10^{-3}	−0.02	0.02	0.24	−0.16	0.07	0.01
5	1289975	rs74682426	a	−0.08	0.02	5.71×10^{-4}	−0.05	0.04	0.17	−0.07	0.03	0.01	−0.29	0.10	3.45×10^{-3}
5	1290319	rs62332591	t	−0.06	0.01	2.33×10^{-5}	−0.08	0.02	9.71×10^{-4}	−0.04	0.02	0.04	−0.21	0.07	1.51×10^{-3}
5	1291735	rs56158232	a	0.02	0.02	0.29	0.02	0.03	0.48	0.01	0.02	0.72	0.15	0.08	0.08
5	1291740	rs56023411	t	0.03	0.02	0.14	0.02	0.03	0.48	0.02	0.02	0.36	0.15	0.08	0.08
5	1292983	rs2853672	a	0.07	0.01	2.37×10^{-6}	0.08	0.02	6.42×10^{-4}	0.05	0.02	0.01	0.22	0.07	8.88×10^{-4}
5	1294086	rs2736098	t	−0.05	0.01	2.01×10^{-3}	−0.08	0.02	1.76×10^{-3}	−0.02	0.02	0.27	−0.14	0.08	0.06
5	1295349	rs2853669	a	0.04	0.01	4.86×10^{-3}	0.08	0.02	2.25×10^{-3}	0.02	0.02	0.33	0.09	0.07	0.22
5	1296072	rs7712562	a	−0.08	0.02	5.28×10^{-4}	−0.05	0.04	0.21	−0.08	0.03	7.51×10^{-3}	−0.30	0.10	3.20×10^{-3}
5	1296486	rs2735940	a	−0.06	0.01	6.96×10^{-6}	−0.07	0.02	4.05×10^{-3}	−0.05	0.02	7.07×10^{-3}	−0.23	0.07	7.60×10^{-4}
5	1296759	rs2736109	t	−0.04	0.02	5.36×10^{-3}	−0.08	0.03	2.75×10^{-3}	−0.02	0.02	0.23	−0.02	0.07	0.79
5	1297258	rs6554754	t	−0.07	0.02	3.92×10^{-3}	−0.04	0.04	0.34	−0.07	0.03	0.02	−0.28	0.11	0.01
5	1297488	rs2736108	t	−0.05	0.02	1.18×10^{-3}	−0.08	0.03	2.87×10^{-3}	−0.03	0.02	0.13	−0.10	0.07	0.16
5	1297854	rs2736107	t	−0.04	0.02	5.91×10^{-3}	−0.05	0.03	0.04	−0.03	0.02	0.11	−0.09	0.07	0.22
5	1297918	rs7449190	t	−0.08	0.02	3.17×10^{-4}	−0.08	0.04	0.03	−0.06	0.03	0.03	−0.30	0.10	3.20×10^{-3}
5	1299859	rs13174814	c	0.01	0.01	0.32	−0.02	0.02	0.36	0.03	0.02	0.16	0.18	0.08	0.02
5	1300310	rs4975612	t	0.01	0.01	0.57	−0.01	0.02	0.63	0.01	0.02	0.57	0.19	0.08	0.02
5	1343794	rs10462706	t	0.01	0.01	0.35	−0.02	0.02	0.43	0.03	0.02	0.14	0.15	0.09	0.10
15	28196145	rs76930569	t	0.04	0.01	8.49×10^{-3}	0.03	0.02	0.20	0.04	0.02	0.02	0.26	0.71	0.72
15	28197037	rs1800414	t	−0.04	0.01	9.10×10^{-3}	−0.03	0.02	0.19	−0.04	0.02	0.02	−0.26	0.71	0.72

Abbreviations: BP, base position; CHR, chromosome; EAF, effect allele frequency; IBD, identity by descent; NSPT, National Survey of Physical Traits; SE, standard error; SL, solar lentigines; TZL, Taizhou longitudinal cohort.

Supplementary Table S24. Heterogeneity (I^2, Q) Measures of Non-facial SL–Associated SNPs in Samples with IBD < 0.1875

			Nonfacial SL			Facial SL		
CHR	BP	SNP	I^2	Q	P_{HET}	I^2	Q	P_{HET}
5	1276050	rs113136187	15.10	2.36	0.31	0.00	1.27	0.53
5	1279790	rs10069690	0.00	1.48	0.48	8.50	2.19	0.34
5	1279964	rs10054203	36.10	3.13	0.21	0.00	0.39	0.82
5	1280028	rs2242652	31.30	2.91	0.23	29.70	2.85	0.24
5	1280128	rs7734992	36.10	3.13	0.21	2.90	2.06	0.36
5	1280830	rs4975538	0.00	1.93	0.38	0.80	2.02	0.36
5	1280938	rs6897196	0.10	2.00	0.37	0.00	1.40	0.50
5	1282319	rs7726159	4.90	2.10	0.35	0.00	1.64	0.44
5	1283312	rs7713218	28.70	2.80	0.25	7.10	2.15	0.34
5	1283486	rs7717443	23.50	2.62	0.27	0.00	1.74	0.42
5	1283755	rs72709458	66.60	5.99	0.05	65.70	5.83	0.05
5	1284135	rs4449583	27.70	2.77	0.25	0.00	1.80	0.41
5	1285162	rs10866498	41.50	3.42	0.18	0.00	1.54	0.46
5	1285974	rs7705526	58.00	4.76	0.09	63.20	5.43	0.07
5	1286516	rs2736100	72.50	7.27	0.03	80.40	10.22	0.01
5	1287194	rs2853677	56.10	4.55	0.10	70.00	6.67	0.04
5	1287505	rs7710703	70.70	6.83	0.03	75.90	8.31	0.02
5	1289880	rs62332588	69.90	6.64	0.04	65.90	5.87	0.05
5	1289975	rs74682426	71.70	7.06	0.03	59.60	4.95	0.08
5	1290319	rs62332591	68.60	6.37	0.04	71.90	7.12	0.03
5	1291735	rs56158232	38.80	3.27	0.19	24.70	2.66	0.27
5	1291740	rs56023411	62.60	5.35	0.07	11.50	2.26	0.32
5	**1292983**	**rs2853672**	**67.10**	**6.09**	**0.05**	**71.00**	**6.91**	**0.03**
5	1294086	rs2736098	19.10	2.47	0.29	59.10	4.89	0.09
5	1295349	rs2853669	11.20	2.25	0.32	47.50	3.81	0.15
5	1296072	rs7712562	55.30	4.47	0.11	61.80	5.24	0.07
5	1296486	rs2735940	61.10	5.14	0.08	69.20	6.49	0.04
5	1296759	rs2736109	0.00	1.00	0.61	25.90	2.70	0.26
5	1297258	rs6554754	40.00	3.33	0.19	53.50	4.30	0.12
5	1297488	rs2736108	0.00	0.27	0.87	21.10	2.54	0.28
5	1297854	rs2736107	0.00	0.18	0.92	0.00	0.80	0.67
5	1297918	rs7449190	54.70	4.41	0.11	61.60	5.21	0.07
5	1299859	rs13174814	0.00	1.96	0.38	72.20	7.19	0.03
5	1300310	rs4975612	5.90	2.13	0.35	64.70	5.66	0.06
5	1343794	rs10462706	0.00	0.90	0.64	56.20	4.57	0.10
15	28196145	rs76930569	0.00	1.65	0.44	0.00	0.26	0.88
15	28197037	rs1800414	0.00	1.51	0.47	0.00	0.23	0.89

Abbreviations: BP, base position; CHR, chromosome; IBD, identity by descent; SL, solar lentigines.
Boldfaces indicate the top SNP associated with nonfacial SL in our study.